2015-06-01

HMGB1 and Ceramides: Potential Mediators of Cigarette Smoke-induced Metabolic Dysfunction

Mikayla Orton Thatcher
Brigham Young University

HMGB1 and Ceramides: Potential Mediators of Cigarette Smoke-Induced Metabolic Dysfunction

Mikayla Orton Thatcher

A dissertation submitted to the faculty of
Brigham Young University
in partial fulfillment of the requirements for the degree of

Doctor of Philosophy

Benjamin T. Bikman, Chair
Paul R. Reynolds
Juan A. Arroyo
Julianne H. Grose
Robert D. Hyldahl

Department of Physiology and Developmental Biology

Brigham Young University

June 2015

ABSTRACT

HMGB1 and Ceramides: Potential Mediators of
Cigarette Smoke-Induced Metabolic Dysfunction

Mikayla Orton Thatcher
Department of Physiology and Developmental Biology, BYU
Doctor of Philosophy

While cigarette smoking is a common-knowledge way to stay lean, it has long been known as a risk factor for diabetes and obesity. Here we establish that smoking causes fat gain and metabolic disruption in mice, effects which are exacerbated by a high-fat, high-sugar diet. We found that smoke exposure increases levels of ceramide—the lipid responsible for diet-induced insulin resistance—and that blocking ceramide production with the pharmacological inhibitor myriocin restored insulin sensitivity, stopped weight gain, and rescued mitochondrial respiration *in vivo* and *in vitro*.

We also sought to assess the impact of the RAGE ligand HMGB1 on skeletal muscle metabolism. We found that respiration between vehicle and HMGB1-injected red gastrocnemius was comparable. In myotubes, adding myriocin treatment to the HMGB1 cells increased respiration above HMGB1 treatment alone. HMGB1 increased oxidative stress in cultured myotubes and increased the transcript levels of Spt2, the enzyme responsible for the rate-limiting step in ceramide synthesis, although transcript levels of markers of mitochondrial fission and fusion leave us unsure of HMGB1's impact on mitochondrial dynamics. HMGB1, even at an exceptionally low dose over only 2 weeks, did cause significant impairment in glucose and insulin tolerance tests. Considering HMGB1's accessibility as a therapeutic target, its involvement in metabolic disruption is worth pursuing further.

Keywords: ceramide, HMGB1, RAGE, cigarette smoking, metabolic dysfunction, myriocin

ACKNOWLEDGMENTS

Will Winder and John Bell had nothing to do with this project, but they are the people who kindled my love for science and directed me into Benjamin Bikman's care. Ben, thank you for your patient guidance and for gradually teaching me to think for myself. Scientifically speaking, a huge thanks to Melissa Hansen for showing me how to do everything and to Trevor Tippetts, Mike Nelson, Duane Winden, and Adam Swensen for lending their expertise from time to time. Thanks to my parents and parents-in-law, who don't quite know what it is that I do, but are terribly proud and supportive anyway. Thanks to my daughter, Jane, who took naps and bottles and smiled through it all. Most importantly, all my love and gratitude to my husband Nate, who made everything possible. I'm not sure if you can dedicate a dissertation, but this one is definitely for him.

TABLE OF CONTENTS

LIST OF FIGURES

CHAPTER 1: Review of the Literature

The cost of diabetes in the United States rose 40% from 2007 to 2013: from $174 billion to $245 billion annually. While that number included direct healthcare costs and productivity lost due to morbidity, disability, and mortality, it could only include diagnosed diabetic patients. By one estimate a third of Americans will have frank diabetes within 40 years (Boyle, Thompson et al. 2010). A large majority of these cases will be type 2 diabetes, separated from type 1 by an excess, rather than an insufficiency, of insulin.

Metabolic syndrome is a term used to describe the constellation of conditions—increased blood pressure, high blood sugar, excess abdominal fat, abnormal cholesterol levels—that come together to drastically increase the risk of heart disease and diabetes. Several important lines of data support the idea that insulin resistance is actually at the root of the metabolic syndrome. Prospective data from the San Antonio Heart Study, for example, showed that patients developed hyperinsulinemia *before* other aspects of the syndrome (Haffner, Valdez et al. 1992). In rodents, a high-fat high-sugar diet caused insulin resistance and hyperinsulinemia quickly—within just a few weeks and before abdominal fat expanded or weight increased (Barnard, Roberts et al. 1998).

Insulin resistance impairs glucose uptake in muscle and excess endogenous glucose from the liver so that blood glucose is abnormally high whether tested in fasted or postprandial animals. Insulin action on lipid and protein metabolism is also impaired: lipolysis slows in adipocytes and protein synthesis decreases in muscle to the point of causing sarcopenia (Jo, Gavrilova et al. 2009; Kawai, de Paula et al. 2012). Additionally, insulin resistance impacts the function of blood vessels, the brain, the pancreas, bone, and beyond. While it is possible for genetic defects in the components of the insulin-signaling cascade to cause insulin resistance,

that etiology is extremely rare. Excess bioactive lipid accumulation and altered substrate handling cause chronic subclinical tissue inflammation and contribute to insulin resistance by inhibiting key phosphorylation events and protein-protein interactions (Schmitz-Peiffer 2002; Turban and Hajduch 2011).

Smoking and Insulin Resistance

Diet is a vital modifiable risk factor for insulin resistance, but it is not the only focal point. Dr. Gerald Reaven first observed over 20 years ago that cigarette smokers tend to be insulin resistant as compared to non-smokers (Reaven and Chen 1992). While his discovery potentially explains how smoking causes dyslipidemia, hypertension, atherosclerosis (DeFronzo and Ferrannini 1991), and hepatic steatosis (Bailey, Mantena et al. 2009; Azzalini, Ferrer et al. 2010; Hamabe, Uto et al. 2011), no data from the ensuing decades have firmly established a causal relationship between cigarette smoking and insulin resistance, let alone a molecular mechanism. Smoking is known, however, to have other effects on metabolism, compromising mitochondrial function in lung and other tissue (Smith, Cooper et al. 1993; Miro, Alonso et al. 1999; Raij, DeMaster et al. 2001; Knight-Lozano, Young et al. 2002; Agarwal, Yin et al. 2014). Today, when three of the top ten killers (heart disease, stroke, and diabetes (Haslam and James 2005; Jha 2009) are linked to insulin resistance and annual cigarette consumption is higher than ever (Eriksen 2012; Troost, Barondess et al. 2012) the correlation Reaven and others described demands further investigation.

In spite of conventional wisdom regarding the leanness of smokers, data suggest that cigarette smoking instead contributes to obesity. The incidence of smoking and obesity mirror each other in nations across the globe—where one factor is increasing, the other follows (Jha 2009; Troost, Barondess et al. 2012). Many investigators speculate a causative association

between exposure to inhaled toxins and metabolic disruption leading to fat gain (Bray and Champagne 2005; Bergman, Perreault et al. 2012; Rajagopalan and Brook 2012; CDCP 2014) adding another layer of complexity to the search for a treatment for obesity and its comorbidities. While cigarette smoke contains chemicals that reportedly increase energy expenditure and promote weight loss (Hofstetter, Schutz et al. 1986), smoke exposure is associated with increased visceral adipose accumulation (Barrett-Connor and Khaw 1989; Shimokata, Muller et al. 1989; Speizer 1992; Simon, Seeley et al. 1997; Jee, Lee et al. 2002; Bamia, Trichopoulou et al. 2004) which increases with greater smoking frequency (Shimokata, Muller et al. 1989). The loss of mitochondrial function as ceramide levels increase may compromise the cells' ability to use fat for fuel. A ceramide-mediated connection between smoking and obesity is also likely because insulin resistance and hyperinsulinemia are common features attending regular smoking (Reaven and Chen 1992; Attvall, Fowelin et al. 1993; Eliasson, Attvall et al. 1994; Eliasson, Mero et al. 1997; Reaven and Tsao 2003; Sonmez, Dogru et al. 2006; Chiolero, Faeh et al. 2008), and insulin is a potent inducer of adipocyte expansion and fat gain (Hustvedt and Lovo 1972; Cox and Powley 1977; King, Smith et al. 1984; Torbay, Bracco et al. 1985; Carlson and Campbell 1993; Makimattila, Nikkila et al. 1999; Velasquez-Mieyer, Cowan et al. 2003).

In the United States alone, 2.5 million people over the last 50 years have died from the known effects of secondhand smoke exposure (CDCP 2014) but the conditions included in that statistic may expand considerably if smoking adds to metabolic morbidity. Certain traffic-related pollutants may also contribute to impaired glucose metabolism and the development of type 2 diabetes mellitus, though not all related studies have observed an association (Brook, Jerrett et al. 2008; Krämer, Herder et al. 2010; Pearson, Bachireddy et al. 2010; Dijkema,

Mallant et al. 2011; Andersen, Raaschou-Nielsen et al. 2012). Metabolic disturbance from inhaled particles may even be responsible for some of the negative outcomes seen in the offspring of women exposed to cigarette smoke or heavy pollution during pregnancy.

Inflammation and Insulin Resistance

Case studies scattered throughout the last 150 years have shown that high doses of anti-inflammatory drugs—sodium salicylates and aspirin—ameliorate symptoms of type 2 diabetes (Williamson 1901; Ebstein 2002; Shoelson, Lee et al. 2003). After the discovery of insulin, the obvious focus was aspirin's impact on insulin secretion, but in 2003, the target of the salicylates was finally determined to be the NFκB axis. (Yuan, Konstantopoulos et al. 2001; Hundal, Petersen et al. 2002; Shoelson, Lee et al. 2003).

Epidemiological studies have long shown that a wide variety of inflammatory markers and mediators, including fibrinogen, CRP, IL-6, and white blood cell count correlate with type 2 diabetes. There are also many published observations of insulin resistance in septic patients (Clowes, Martin et al. 1978; Raymond, Harkema et al. 1981; Iochida, Tominaga et al. 1989; Shangraw, Jahoor et al. 1989) and high circulating cytokines in patients with obesity and diabetes (Pickup and Crook 1998; Visser, Bouter et al. 1999; Yudkin 2000). Rodent and human models both demonstrated increased adipose TNF-α in insulin resistant states (Hotamisligil, Shargill et al. 1993; Hotamisligil, Arner et al. 1995; Kern, Saghizadeh et al. 1995) However, the eventual discovery that exogenous TNF-α (an inflammatory cytokine) could *induce* insulin resistance was a major turning point in elucidating the etiology of type 2 diabetes (Shoelson, Lee et al. 2003). Studies blocking TNF-α specifically have thus far been inconclusive (Dominguez, Storgaard et al. 2005; Gonzalez-Gay, De Matias et al. 2006), but there are a number of inflammatory molecules that may make useful treatment targets. Many proinflammatory stimuli

activate multiple pathways simultaneously, but genetic or chemical inhibition of any of them can improve insulin resistance. Thus, researchers in this field have begun to restructure their thinking away from individual cytokines to inflammatory pathways and their activators. Positive feedback loops abound in these systems, adding complexity to our models (Shoelson, Lee et al. 2003). Obesity and high-fat diet have been shown to activate IKKβ and JNK pathways in adipose, liver, and macrophages. Scott Summers' lab attributes this IKKβ and JNK activation to TLR4-induced ceramide accumulation (Holland, Bikman et al. 2011), showing that when ceramide accumulation is blocked in a murine model, diet-induced insulin resistance does not develop (Cai, Yuan et al. 2005; Sims, Rowe et al. 2010). Ceramide also interferes with Akt phosphorylation, directly disrupting the insulin signaling pathway to cause insulin resistance.

Ceramide

When fatty acids enter a cell, they are promptly esterified with coenzyme A to form acyl-CoA's. When transferred to a glycerol backbone, they form mono-, di-, and tri-acylglycerals. Alternatively, the acyl-CoA esterifies with sphingosine to form ceramides. Ceramides are a type of sphingolipid that, while found primarily in cell membranes (Turinsky, Bayly et al. 1990), regulate a variety of cellular processes including apoptosis, stem cell differentiation, and cell polarity (Bieberich 2011). Sphingolipids were named for the mysterious sphinx, but as knowledge of them expands they are more notable for being the most pathogenic of lipids (Summers 2006), despite how little they make up of total lipids. Ceramide is of interest as a potential mediator of cigarette smoke-induced insulin resistance because its accumulation in skeletal muscle has been shown to impede insulin signaling in obesity-induced insulin resistance. Increased ceramide in liver and muscle was associated with insulin resistance in obese Zucker rats (Turinsky, Bayly et al. 1990). Levels of endogenous sphingolipids are doubled in insulin-

resistant obese subjects compared to lean subjects, whether sedentary or exercise trained (Amati, Dube et al. 2011).

A workhorse tool in the study of ceramides in obesity-induced insulin resistance is the use of myriocin. Myriocin potently inhibits the enzyme serine palmitoyltransferase (SPT), which catalyzes the first step of sphingolipid biosynthesis (Miyake, Kozutsumi et al. 1995). This inhibition is dose-dependent and has been shown to be highly specific. In the work described in the prior paragraph, for example, myriocin was used to show that ceramide depletion prevented insulin resistance in high fat fed mice.

Various stress stimuli have already been shown to increase ceramide synthesis [(Holland, Knotts et al. 2007)], and cigarette smoke has been shown to promote ceramide production in the lungs (Levy, Khan et al. 2009; Goldkorn and Filosto 2010).

Cigarette smoking also upregulates the receptor for advanced glycation end products (RAGE) and triggers an inflammatory state through activating the small GTPase Ras and the transcription factor NFκB (Reynolds, Kasteler et al. 2011) Other inducers of NFκB include increased reactive oxygen species (ROS) and tumor-necrosis factor alpha (TNFα), so RAGE and TLR4 can be considered converging pathways (Cai, Yuan et al. 2005).

TLR4 is a pattern recognition receptor whose inflammatory roles and ligands overlap strongly with those of RAGE, which is also activated in diet-induced obesity. Interestingly, TLR-4 knockout mice are protected from ceramide accumulation and insulin resistance following palmitate infusion (Holland, Knotts et al. 2007).

A ceramide-centric mechanism would tie together the mitochondrial dysfunction seen in smoking and insulin resistance—ceramide inhibits electron transport chain intermediates and promotes oxidative stress (Bikman and Summers 2011).

Receptor for Advanced Glycation End Products

The receptor for Advanced Glycation End Products (RAGE) was originally named and classified as a scavenger receptor vital for clearing outmoded proteins, lipids, and nucleic acids tagged by glycation for degradation. (Vlassara, Brownlee et al. 1985; Vlassara, Bucala et al. 1994) This notion was turned on its head when RAGE was first cloned for study—the binding of AGEs to RAGE resulted in prolonged inflammation rather than quicker clearance of old macromolecules. The original conception of RAGE has also expanded to include its binding to non-AGE ligands, including molecules such as amyloid-β peptide, amyloid A, S100s, and HMGB1, that are pro-inflammatory and tend to accumulate in tissues during aging and chronic degenerative diseases. (Bierhaus, Schiekofer et al. 2001; Treutiger, Mullins et al. 2003). RAGE ligands share common tertiary structures (beta sheets, fibrils, etc.) rather than specific secondary structures (Schmidt, Yan et al. 2001; Bucciarelli, Wendt et al. 2002). RAGE is unique among pattern recognition receptors in its interacting mainly with endogenous molecules (Musumeci, Roviello et al. 2014).

RAGE-ligand binding has been linked to many of the major signaling cascades—NF-κB, ERK1/2, JNK, JAK/STAT—and whether different RAGE ligands activate different downstream pathways (within a cell or depending on cell type) is an outstanding question in this field. Exogenous soluble RAGE—acting as a decoy—has protective effects in mice with or without RAGE, suggesting that RAGE ligands must recognize several receptors: this question too requires further research. Skin and lung cells express RAGE constitutively throughout adulthood, but RAGE upregulation in other adult cell types appears to require ligand accumulation or transcription factor activation, both of which would happen in response to stress (Brett, Schmidt et al. 1993; Bierhaus, Humpert et al. 2005). RAGE engagement begins a signaling cascade

leading to IkBa phosphorylation and degradation, allowing free NFkB to translocate into the nucleus. Once there NFkB activates transcription of NFkB-regulated target genes. Some of these—Bcl-XL, Bcl-2, Bcl-2 homologues A1—are anti-apoptotic and promote cellular survival under stress. Others—cytokines, adhesion molecules, prothrombotic and vasocontrictive gene products—are less helpful. NFkB also promotes transcription of RAGE itself, creating a positive feedback loop (Barnes and Karin 1997; Li and Schmidt 1997; Bierhaus, Schiekofer et al. 2001; Bierhaus, Humpert et al. 2005).

High-Mobility Group Box Protein 1

HMGB1 is a chromatin-associated protein present in the nuclei of almost all eukaryotic cells (Goodwin, Sanders et al. 1973) and named for its high electrophoretic mobility. Its physiologic role is to maintain nucleosome structure (Müller, Scaffidi et al. 2001) and regulate gene transcription (Thomas 2001). The 215-amino acid protein consists of an A box and a B box, which interact with DNA to bend the double helix in a non-sequence-specific way (Read, Cary et al. 1993; Weir, Kraulis et al. 1993; Hardman, Broadhurst et al. 1995), and a c-terminus that contributes to spacing and regulation (Wang, Zeng et al. 2007).

Necrotic cells release HMGB1 passively (Scaffidi, Misteli et al. 2002) and various cells secrete it actively in response to stress stimuli (Gardella, Andrei et al. 2002; Bonaldi, Talamo et al. 2003; Semino, Angelini et al. 2005; Ito, Fukazawa et al. 2007; Gougeon and Bras 2011). Once outside the cell, HMGB1's function is dramatically different—it participates in regulating inflammatory processes (Wang, Bloom et al. 1999) as a damage-associated molecular pattern molecules (DAMP), which can bind to and activate pattern recognition receptors to induce a noninfectious inflammatory response (Kuipers, van der Poll et al. 2011). RAGE and TLR4 are the two major types of mediating receptors (Sims, Rowe et al. 2010); HMGB1 is known

primarily as a RAGE ligand as the HMGB1-RAGE interaction has been shown to be specific, saturable, dose-dependent, and of higher affinity than RAGE-AGE interactions (Hori, Brett et al. 1995). A number of TLR ligands, including LPS, form complexes with HMGB1 that provoke stronger inflammatory responses than either partner molecule alone (Tian, Avalos et al. 2007; Hreggvidsdottir, Ostberg et al. 2009; Qin, Dai et al. 2009). These synergistic responses appear to involve co-activation of both TLR and RAGE. High serum levels of HMGB1 have been observed in such varied disease states as sepsis, rheumatoid arthritis, chronic kidney disease, systemic lupus erythematosis, cancer, diabetes, and Alzheimer's (Musumeci, Roviello et al. 2014). Whether that is a contributing factor, a negative side effect, or a helpful survival response remains to be seen for each pathology.

HMGB1 stands out among inflammatory cytokines as an accessible treatment target because of its late induction in inflammation (Wang, Bloom et al. 1999). Already, several means have been shown to effectively block HMGB1 or its interaction with RAGE, including competitive inhibition using truncated HMGB1 along with a variety of natural and synthetic small molecules (Musumeci, Roviello et al. 2014).

Myriocin

While complete knockouts of ceramide-synthesizing enzymes are lethal and tissue-specific knockouts have yet to be developed, the drug myriocin is a useful tool in loss-of-function experiments.

Myriocin is an antibiotic produced by some thermophilic fungi (Hojjati, Li et al. 2005). It is an immunosuppressant reported to be 10-100 fold stronger than ciclosporin and targets serine palmitoyltransferase (SPT), the enzyme that catalyzes the first step of sphingolipid biosynthesis (Miyake, Kozutsumi et al. 1995). Myriocin is an analog of sphingosine, which is a component of

all sphingolipids, and is thought to act either by altering normal sphingolipid metabolism or by interacting with sphingolipid binding sites in regulatory processes (Shier 2000). Myriocin is frequently used to experimentally reduce ceramide synthesis *in vitro* and *in vivo.* Myriocin has been shown to reduce insulin resistance, oxidative stress, and pro-inflammatory cytokines (Tong, Longato et al. 2014). While off-target effects of pharmacological agents are always a concern, CHO cell mutants defective in SPT have exactly the same phenotype as cells treated with myriocin: the drug seems to be exceptionally target specific (Hanada, Nishijima et al. 2000).

CHAPTER 2: Ceramides Mediate Cigarette Smoke-Induced Metabolic Disruption in Mice

Abstract

Cigarette smoke exposure increases lung ceramide biosynthesis and alters metabolic function. We hypothesized that ceramides are released from the lung during cigarette smoke exposure and result in elevated skeletal muscle ceramide levels, resulting in insulin resistance and altered mitochondrial respiration. Employing cell and animal models, we explored the effect of cigarette smoke on muscle cell insulin signaling and mitochondrial respiration. Muscle cells were treated with conditioned media from cigarette smoke extract (CSE)-exposed lung cells, followed by analysis of ceramides and assessment of insulin signaling and mitochondrial function. Mice were exposed to daily cigarette smoke and high-fat, high-sugar (HFHS) diet with myriocin injections to inhibit ceramide synthesis. Comparisons were conducted between these mice and control animals on standard diets in the absence of smoke exposure and myriocin injections. Muscle cells treated with CSE-exposed conditioned medium were completely unresponsive to insulin stimulation and mitochondrial respiration was severely blunted. These effects were mitigated when lung cells were treated with the ceramide inhibitor myriocin prior to and during CSE exposure. In mice, daily cigarette smoke exposure and HFHS diet resulted in insulin resistance, which correlated with elevated ceramides. While myriocin injection was protective against insulin resistance with either smoke or HFHS, it was insufficient to prevent insulin resistance with combined CS and HFHS. However, myriocin injection restored muscle mitochondrial respiration in all treatments. Ceramide inhibition prevents metabolic disruption in muscle cells with smoke exposure and may explain whole-body insulin resistance and mitochondrial dysfunction *in vivo*.

Introduction

Obesity and cigarette smoking are two of the largest causes of preventable deaths worldwide, increasing the risk of multiple illnesses such as heart disease, stroke, airway infections, and diabetes (Jha 2009; World Health Organization 2012). The incidence of smoking and obesity mirror each other in nations across the globe—where one risk factor is increasing, the other follows (Jha 2009; World Health Organization 2012). This correlation has elicited speculation of a causative association between toxin exposure, such as cigarette smoke, and metabolic disruption (Bray and Champagne 2005; Bergman, Perreault et al. 2012; Rajagopalan and Brook 2012), which adds another layer of complexity to the already convoluted search for a treatment to obesity and its comorbidities. While cigarette smoke contains chemicals that reportedly increase energy expenditure and promote weight loss (Hofstetter, Schutz et al. 1986), smoke exposure is associated with increased visceral adipose accumulation (Shimokata, Muller et al. 1989; Speizer 1992) that increases with greater smoking frequency (Shimokata, Muller et al. 1989).

Two lines of evidence may support the theory that cigarette smoke causes metabolic disruption leading to fat gain. First, cigarette smoke exposure is known to disturb mitochondrial function and biogenesis (Miro, Alonso et al. 1999; Agarwal, Yin et al. 2014), which may compromise the cell's ability to use fat for fuel. Second, insulin resistance and hyperinsulinemia are common features attending regular smoking (Reaven and Chen 1992; Attvall, Fowelin et al. 1993; Eliasson, Mero et al. 1997; Reaven and Tsao 2003; Chiolero, Faeh et al. 2008), and insulin is a potent inducer of adipocyte expansion and fat gain (Hustvedt and Lovo 1972; Makimattila, Nikkila et al. 1999; Velasquez-Mieyer, Cowan et al. 2003). How smoke exposure causes both of these deleterious metabolic consequences is unclear. Of the myriad mediators that may disrupt

healthy metabolic function in response to cigarette smoke exposure, the particular effects of the sphingolipid ceramide on cellular insulin sensitivity and mitochondrial function elucidate a novel mechanism and potential therapeutic target (Bikman and Summers 2011).

The lung produces ceramides in response to cigarette smoke exposure (Levy, Khan et al. 2009; Goldkorn and Filosto 2010), which may explain the altered metabolic function evident with smoking (Du, Wang et al. 2009; Bikman 2012). Ceramide is a well-established mediator of both insulin resistance (Chavez, Knotts et al. 2003; Summers 2006) and compromised mitochondrial function (Gudz, Tserng et al. 1997; Smith, Tippetts et al. 2013). Based on these observations, the purpose of our study was to test the hypothesis that cigarette smoke exposure leads to ceramide accumulation in systemic tissues, particularly skeletal muscle, and mediates insulin resistance and altered mitochondrial function. Additionally, by using a rodent smoke-exposure model, these studies provide evidence that long-term cigarette smoke exacerbates weight gain.

Materials and Methods

Cell Culture

Cigarette smoke extract (CSE) was generated as previously described with slight modifications (Reynolds, Cosio et al. 2006). Briefly, one 2RF4 research cigarette (University of Kentucky, Lexington, KY) was continuously smoked by connecting the filtered end of the cigarette to a vacuum pump, pulling the particles into 5 ml of DMEM/F12 and the resulting medium was defined as 100% CSE and diluted with culture medium to 10%. The total particulate matter content of 2RF4 cigarettes is 11.7 mg/cigarette, tar is 9.7 mg/cigarette, and nicotine is 0.85 mg/cigarette. Human type II–like pulmonary adenocarcinoma cells (A-549) were maintained in DMEM/F12 supplemented with 10% FBS (Invitrogen) and antibiotics. Cells

were split into 6-well dishes and grown to 80% confluence. C2C12 muscle cells were maintained in DMEM + 10% FBS. For differentiation into myotubes, myoblasts were grown to confluency and the medium was replaced with DMEM + 10% horse serum (Invitrogen, Grand Island, NY). Myotubes were used for experiments on day 4 of differentiation. A-549 cultures were exposed to serum-free media supplemented with 10% CSE or media alone for 4 h, after which the medium was transferred to differentiated C2C12 myotubes (termed "conditioned medium") for 12 h. Where indicated, cells were treated with myriocin (10 μM, Sigma, M1177). Muscle cells were harvested for RNA, protein, and lipid isolation following treatments.

Animals

Male C57Bl6 mice were housed in a conventional animal house and maintained on a 12-hour light–dark cycle. Two animal studies were conducted. In the first study, animals received standard diet chow (Harlan Teklad 8604) and water *ad libitum*. At 12-14 wk of age, animals were randomly divided into room air and cigarette smoke (CS)-exposed groups. Mice were placed in soft restraints and connected to the exposure tower of a nose-only exposure system (InExpose System, Scireq, Canada). Animals were nasally exposed to mainstream CS generated by research cigarettes where a computer-controlled puff was generated every minute, leading to 10 s of CS exposure followed by 50 s of fresh air. The CS-exposed group inhaled CS from two consecutive cigarettes per day for three weeks, at which point the dosage was increased to two cigarettes twice daily. Control animals were similarly handled and restrained in fresh air for the same duration. After the 6-wk course, mice underwent i.p. glucose (G7021; Sigma-Aldrich, St. Louis, MO) and insulin (Actrapid; Novo Nordisk, Plainsboro, NJ) tolerance tests. For both tests, mice were fasted for 6 hours and received an injection of either glucose (1 g/kg body weight) or insulin (0.75 U/kg body weight). Blood glucose was determined at the times indicated in the

figures, using the Bayer Contour glucose meter. For the second study, 12-wk-old mice were separated into one of several treatment groups for 8 wk. Each of the following groups were duplicated to have one group receive vehicle or myriocin injections (0.3 mg/kg) every other day for a total of eight groups: 1) control – standard diet chow, no smoke; 2) cigarette smoke exposure (two cigarettes, twice daily) with standard diet chow; 3) high-fat, high-sugar diet (Harlan Teklad 45F30S); 4) high-fat, high-sugar diet with cigarette smoke exposure. Tissues were harvested at the conclusion of the study period and following a 6-hr fast. Insulin resistance was assessed using fasting blood glucose and insulin (MP Biomedicals, Insulin RIA kit, 07260102) to compute a homeostatic model assessment score, as previously described (Bikman, Guan et al. 2012). Studies were conducted in accordance with the principles and procedures outlined in the National Institutes of Health Guide for the Care and Use of Laboratory Animals and were approved by the Institutional Animal Care and Use Committee (IACUC) at Brigham Young University.

Lipid Analysis

Lipids were extracted and quantified as described previously (Smith, Tippetts et al. 2013). Briefly, lipids were isolated with chloroform/methanol (1:2), and after addition of water, the organic phase was collected and dried. After resuspension, lipids were quantified using a shotgun lipidomics technique on a Thermo Scientific LTQ Orbitrap XL mass spectrometer.

Protein Quantification and Quantitative Real-time PCR

Protein and message were quantified as described previously (Erickson, Smith et al. 2012; Smith, Tippetts et al. 2013). Primers were used as listed previously (Erickson, Smith et al. 2012). β-actin reactions were performed side by side with every sample analyzed. The following antibodies were used: β-Actin (Cell Signaling; 4967), Akt (9272), pAkt-ser473 (9271),

GSK3β (9315), pGSK3β-ser9 (9323), SPT2 (Santa Cruz; sc-27500), Anti-oxphos complex (Invitrogen; 457999). Changes in mRNA level of each gene following treatments were normalized to the β-actin control mRNA according to Pfaffl (Pfaffl 2001).

Cell and Muscle Fiber Bundle Permeabilization

Cells and tissue were prepared for the mitochondrial respiration assay as described previously (Smith, Tippetts et al. 2013). Following respiration protocol (outlined below), samples were removed from the chambers and used for further analysis, including protein quantification.

Mitochondrial Respiration Protocol

High-resolution O_2 consumption was determined at 37˚C in permeabilized cells and fiber bundles using the Oroboros O_2K Oxygraph (Innsbruck, Austria) with MiR05 respiration buffer as described previously (Pesta and Gnaiger 2012; Smith, Tippetts et al. 2013). Respiration was determined by all or parts of the following substrate-uncoupler-inhibitor-titration (SUIT) protocol (Jheng, Tsai et al. 2012): electron flow through complex I was supported by glutamate+malate (10 and 2 mM, respectively) to determine oxygen consumption from proton leak (GM_L). Following stabilization, ADP (2.5 mM) was added to determine oxidative phosphorylation capacity (GM_P). Where indicated, outer mitochondrial membrane integrity was tested by adding cytochrome *c* (10μM; GMc_P). Succinate was added (GMS_P) for complex I+II electron flow into the Q-junction. To determine full electron transport system (ETS) capacity over oxidative phosphorylation in cells, the chemical uncoupler carbonyl cyanide 4-(trifluoromethoxy) phenylhydrazone (FCCP) was added (0.05 μM, followed by 0.025 μM steps until maximal O_2 flux was reached). Complex II-supported ETS was then measured by inhibiting complex I with rotenone (Rot; 0.5 μM). Lastly, residual oxygen consumption was

measured by adding antimycin A (2.5 μM) to block complex III action, effectively stopping any electron flow. This value provides a rate of respiration that is used as a baseline.

Glycogen Assay

Glycogen was measured from cells where indicated according to the manufacturer's instructions (BioVision Inc.; Milpitas, CA).

Statistics

Data are presented as the mean ± SEM. Data were compared by ANOVA with Tukey's post-hoc analysis (Graphpad Prism; La Jolla, CA). Significance was set at $p < 0.05$.

Results

Alveolar Type 2 Cells Produce and Secrete Ceramide in Response to Cigarette Smoke Extract

Compared to PBS-treated cells, ceramide was significantly elevated in alveolar type 2 A549 cells following treatment with cigarette smoke extract (CSE) for 4 h (Figure 2.1). However, this effect was prevented when CSE-treatment was supplemented with myriocin (CSE+Myr; Figure 2.1). Myriocin inhibits the initial and rate-limiting step in *de novo* ceramide biosynthesis, serine palmityoltransferase (SPT) by preventing condensation of palmitoyl-CoA and serine. The relevance of SPT was further determined by measuring the gene expression of SPT2. CSE treatment elicited an over two-fold increase in SPT2 gene expression and protein (Figure 2.2), providing evidence of the role of the *de novo* pathway in CSE-induced ceramide biosynthesis. In addition to ceramide production, we sought to determine the ability of A549 cells to secrete ceramide. Accordingly, lipids were isolated and ceramides measured following 8 h treatment with PBS- and CSE-medium (+/- myriocin) (Figure 2.3). Medium from CSE-treated

cells contained roughly 60% more ceramide compared to PBS-treated cells. Moreover, CSE-treated cells receiving myriocin did not secrete ceramides greater than control treatments.

Muscle Cells Treated With Lung-cell Conditioned Medium Have higher Ceramide Levels

To determine the effect of lung cell-secreted ceramides on muscle cell ceramide metabolism, conditioned medium from PBS- and CSE-treated cells (+/- myriocin) was harvested from A549 cells and placed on C2C12 myotubes for 12 h, as outlined in Figure 2.4A. Myotubes treated with conditioned medium from CSE-treated cells (SCM) had significantly higher levels of ceramide compared with both myotubes treated with PBS conditioned medium (CCM) as well as addition of myriocin to CSE treatment (SCM+Myr; Figure 2.4B).

Muscle Cells Experience Metabolic Disruption Following CSE Conditioned Medium Treatment

Two important aspects of metabolic disruption that may mediate obesity-related morbidities and/or exacerbate weight gain are the reduction of muscle insulin sensitivity and altered mitochondrial respiration. Similar to above, C2C12 myotubes were treated with conditioned medium from A549 cells previously treated with normal medium, CSE, or CSE+Myr. Following 12-h serum-free conditioned medium treatment, myotubes were stimulated with insulin for 10 min. As an indicator of insulin signaling, Akt and GSK3β phosphorylation was determined. Whereas control-conditioned medium myotubes experienced a marked increase in both Akt and GSK3β phosphorylation in response to insulin, myotubes treated with CSE-conditioned medium failed to respond to insulin (Figures 2.5 and 2.6). However, when myotubes were treated with conditioned medium from A549 cells that were co-treated with myriocin during CSE exposure, insulin responsiveness was restored (Figures 2.5 and

2.6). These results were strengthened by determining glycogen accrual with similar treatments (Figure 2.7).

To determine mitochondrial respiration, following similar treatments indicated above, myotubes were permeabilized to undergo a substrate-uncoupler-inhibitor titration protocol (protocol details provided in Methods). No difference in rates of mitochondrial O_2 was observed between treatment conditions with addition of glutamate and malate (*Leak* state) (Figure 2.8). However, addition of ADP to measure respiration with complex I-mediated oxidative phosphorylation (GM_P) revealed a marked contrast, where O_2 consumption failed to increase in myotubes treated with conditioned medium from CSE-treated A549 cells (SCM). Similar results were found with addition of succinate to introduce complex II-mediated respiration GMS_P, as well as FCCP addition to measure uncoupled respiration (GMS_E). Addition of rotenone (complex I inhibitor) resulted in a general reduction and equalization of respiration rates, regardless of treatment [$S(Rot)_E$]. Addition of myriocin to CSE-treatment completely protected mitochondrial respiration (SCM+Myr) and rates were comparable to control (CCM) throughout the assay. Altogether, these findings suggest a severely compromised ability of muscle cell mitochondria to respire in the midst of the high-ceramide state caused by cigarette smoke. The smoke-induced decrease in mitochondrial respiration may at least partly result from the slight, yet significant ceramide-dependent reduction in complex III and IV protein evident in SCM-treated cells (Figure 2.9).

Cigarette Smoke Exposure Causes Metabolic Disruption In Mice

In an effort to determine whether cigarette smoke causes insulin resistance, adult male mice were exposed to cigarette smoke daily for 6 wk. Treatment period was determined by the length of time necessary to observe differences in glucose tolerance and insulin sensitivity. We

found that smoke-exposed mice became less glucose tolerant (Figure 2.10A) and less insulin sensitive (Figure 2.10B) than control mice. Further, the insulin resistance was attended by altered ceramides—smoke-exposed mice had significantly elevated ceramides in multiple tissues, including skeletal muscle (Figure 2.12). A portion of the gastrocnemius was permeabilized to assess mitochondrial respiration (Figure 2.11). We found that ADP-supported complex I-mediated respiration (GM_P) was significantly blunted in smoked animals. This difference was further exaggerated with succinate addition (GMS_P) to introduce complex II, but was absent with uncoupling by the addition of FCCP (GMS_E), suggesting that maximal, but not submaximal, mitochondrial respiration rate in the muscle is unaffected by cigarette smoke exposure.

Ceramide Inhibition Prevents Smoke-Induced Metabolic Disruption

The previous animal experiment provided proof of concept that cigarette smoke exposure causes insulin resistance. To elucidate the role of ceramides in smoke-induced metabolic disruption, mice received vehicle or myriocin injections every other day to inhibit ceramide biosynthesis. Additionally, mice received a longer smoking regimen with the addition of a dietary intervention. Namely, animals received standard diet (SD) chow or a high-fat, high-sugar (HFHS) diet. The rationale for the dietary intervention was to more closely mimic current real world conditions, considering smokers tend to engage in less healthy eating habits than non-smokers (Hebert and Kabat 1990). Interestingly, cigarette smoke exposure (SD+CS) alone increased body weight (Figure 2.7A), despite no apparent difference in eating habits (Sup. Figure 2.1). The high-fat, high-sugar diet (HFHS) also resulted in significantly higher body weight when compared with animals fed SD, though the combination of HFHS diet and smoke (HFHS +CS) resulted in the highest weight gain among all groups (Figure 2.13A). However, myriocin

injection prevented CS-induced weight gain and mitigated HFHS-induced weight gain, but was insufficient to prevent weight gain with combined HFHS+CS (Figure 2.13A). Ceramides increased in soleus with all interventions (Figure 2.13B). Myriocin injection prevented significant ceramide gains with all treatments. At the conclusion of the study, fasting blood glucose and insulin levels were used to determine HOMA-IR score following the 8-wk treatment period (Figure 2.13C). HOMA-IR scores suggested pronounced insulin resistance with smoke (SD+CS) and dietary intervention (HFHS, HFHS+CS), but this was significantly mitigated with myriocin treatment. Lastly, red gastrocnemius fibers were separated and permeabilized to determine mitochondrial respiration (Figure 2.14). Cigarette smoke (CS) exposure, regardless of diet, blunted mitochondrial respiration throughout the protocol, though inhibition with HFHS diet alone became apparent only after addition of succinate (GMS_P). Myriocin injections failed to prevent reduced respiration with the various treatments, but it offered some protection considering that respiration was generally higher with myriocin than the comparable vehicle-treated conditions.

Discussion

Multiple studies have corroborated a relationship between smoking and insulin resistance since the initial Reaven paper (Attvall, Fowelin et al. 1993; Borissova, Tankova et al. 2004; Ebersbach-Silva, Alves et al. 2013). While previous findings may reveal a mechanism (i.e., insulin resistance) whereby smoking results in systemic diseases (DeFronzo and Ferrannini 1991; Hamabe, Uto et al. 2011), the ensuing decades have failed to implicate a mediating molecular process linking smoking and insulin resistance. In addition to insulin resistance, smoking compromises mitochondrial function (Miro, Alonso et al. 1999; Knight-Lozano, Young et al. 2002; Barreiro, del Puerto-Nevado et al. 2012). The purpose of this report was to

determine the role of the sphingolipid ceramide as a mediator of cigarette smoke-induced metabolic disruption, i.e., insulin resistance and reduced mitochondrial function.

Our first step was to determine whether lung cells, specifically alveolar type 2 cells or bronchial epithelial cells (data not shown), produce and secrete ceramide in response to cigarette smoke extract. We observed that both cells secrete ceramides with smoke exposure, but the response is greater in alveolar type 2 cells. Previous studies exploring the source of blood ceramides have revealed a prominent role for the liver in producing and packaging ceramides into lipoproteins for transport from the liver throughout the body (Contreras, Villar et al. 2003). However, ceramides are able to cross the cell membrane without lipoproteins (Contreras, Villar et al. 2003), which is our predicted mechanism for ceramides exiting lung cells. However, once in the blood, ceramides are likely transported via albumin, or, more likely, lipoproteins (Watt, Barnett et al. 2012). Upon confirming ceramide secretion from lung cells, we utilized a cell culture system of treating myotubes with conditioned medium from alveolar type 2 cells that were treated with cigarette smoke extract with or without myriocin to inhibit ceramide synthesis.

Our findings of a protective effect on insulin signaling and mitochondrial respiration with myriocin-treated lung cells suggest that ceramides are necessary for smoke-induced metabolic disruption *in vitro*. Results from our animal studies are noteworthy considering that chronic smoking caused insulin resistance. Importantly, the dose and method of cigarette smoke exposure we used has been previously shown to yield similar levels of blood carboxyhemoglobin seen in human smokers (Wright, Cosio et al. 2008). To determine the role of ceramides in insulin signaling and mitochondrial function *in vivo,* we performed a second and similar smoking regimen that prolonged the smoke exposure (from 6 to 8 wk), and included a high-fat, high-sugar (HFHS) diet with regular myriocin injections. The rationale for the HFHS diet was to more

closely mimic real world conditions, considering smokers tend to engage in less healthy eating habits than non-smokers (Hebert and Kabat 1990). In general, the combination of cigarette smoke and HFHS diet tended to exacerbate the effects of smoke alone, including body weight, ceramides, and HOMA-IR. Ceramide inhibition with myriocin treatment tended to mitigate these negative effects.

Altogether, our findings build upon initial observations of smoking and disturbed metabolic function (Facchini, Hollenbeck et al. 1992; Reaven and Chen 1992; Chen, Li et al. 2008) and allow, for the first time, a definitive implication of ceramides as a mediator of cigarette smoke-induced metabolic disruption.

Cigarette smoke also elicits a host of negative effects on mitochondria, including inhibition of respiration (Miro, Alonso et al. 1999; Knight-Lozano, Young et al. 2002) and increased ROS generation (Barreiro, del Puerto-Nevado et al. 2012). It is tempting to speculate these effects may be a result of altered mitochondrial dynamics, which is affected by smoke exposure (Gannon, Stampfli et al. 2013). We have recently shown that mitochondrial fission is necessary for ceramide-induced changes in mitochondrial function, including varied respiration and ROS production (Smith, Tippetts et al. 2013).

Cigarette smoke is a common environmental toxin, with half of the U.S. population being regularly exposed (Pirkle, Flegal et al. 1996; Pirkle, Bernert et al. 2006) and approximately 20% of young children living with someone who smokes in the home (2010). Every day, almost 4,000 young adults smoke their first cigarette and 1,000 become habitual smokers (2011). We intentionally utilized sidestream (i.e., second hand) smoke in this study, given that it affects both smokers and bystanders. Our findings, in conjunction with numerous observational studies (Reaven and Chen 1992; Attvall, Fowelin et al. 1993; Eliasson, Mero et al. 1997; Reaven and

Tsao 2003; Chiolero, Faeh et al. 2008) linking smoking with insulin resistance are relevant to current metabolic syndrome and obesity concerns, given that insulin resistance is the crux of the pathologies that constitute the metabolic syndrome (Haffner, Valdez et al. 1992). Previous animal studies have indicated weight loss in smoke-exposed mice (Chen, Vlahos et al. 2005), though the treatment length was considerably shorter than that used in this study (4 d vs. 8 wk).

Whether smoking exerts an anti- or pro-obesogenic effect in humans is unclear. Smoking is traditionally considered to prevent fat gain, but these observations are exclusively cross sectional (Chiolero, Faeh et al. 2008). In contrast, prospective studies following large cohorts reveal that initiation of smoking promotes greater fat gain compared with non-smokers (Speizer 1992) and heavy smoking increases the fat gain (John, Hanke et al. 2005). Given insulin's potent actions in increasing fat mass (Hustvedt and Lovo 1972; Makimattila, Nikkila et al. 1999; Velasquez-Mieyer, Cowan et al. 2003), the hyperinsulinemia that accompanies insulin resistance may be an important regulator of smoke-induced fat gain. Importantly, while cross sectional studies suggest smokers may indeed weigh less (e.g., lower BMI), they also tend to have a higher waist-to-hip ratio (Chiolero, Faeh et al. 2008), suggesting increased visceral fat, which is an additional feature of the metabolic syndrome. Our data suggest that ceramide is an important mediator of the metabolic disruption and weight gain that accompanies chronic smoke exposure.

This study presents the perspective that smoking disrupts healthy metabolic function and, via ceramide accrual, increases risk of weight gain, especially when smoking is combined with a typical Western diet. Future efforts are currently focused on exploring the role of ceramide in other smoke-related pathologies, including the considerable smoke-induced cardiovascular burden. These findings reveal a new metabolic concern for smokers who struggle to quit, but we consider the concern even greater for those exposed to cigarette smoke as bystanders,

particularly at early ages. In the end, the results suggest a potential use for anti-ceramide therapies in preventing at least some of the metabolic consequences of smoke exposure.

Acknowledgments

Trevor Tippetts, Michael Nelson, Madeline Anderson, and Ian Johnson helped with mouse injections. Duane Winden coordinated the smoke machine and assisted with surgeries. Adam Swensen worked tirelessly to analyze lipid samples and Jim Porter helped me design the miniaturized radioimmunoassay. Benjamin Bikman helped with experimental design and measured cellular respiration. Thanks, everybody!

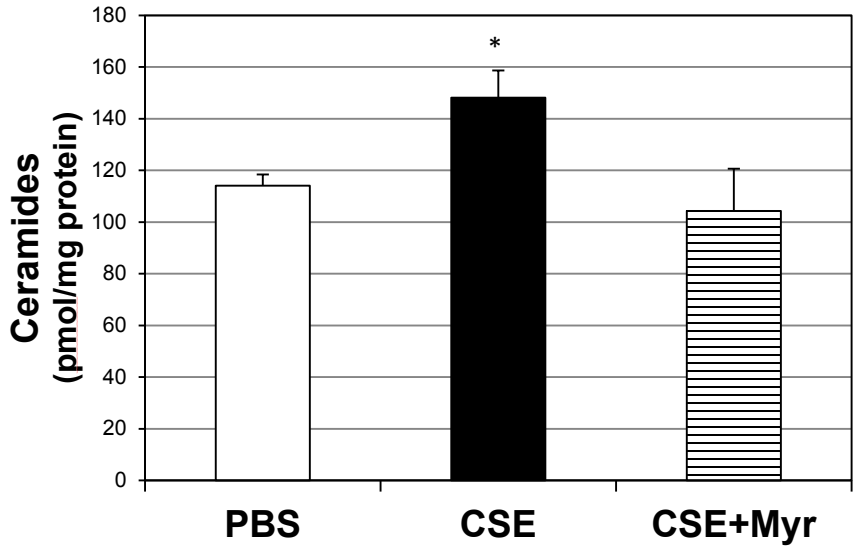

Figure 2.1: Cigarette Smoke Extract Increases Ceramide Biosynthesis.

Alveolar type 2 cells (A549) were treated with PBS or cigarette smoke extract without (CSE) or with myriocin (CSE+Myr) suspended in growth medium. Following treatment period, ceramides were measured.

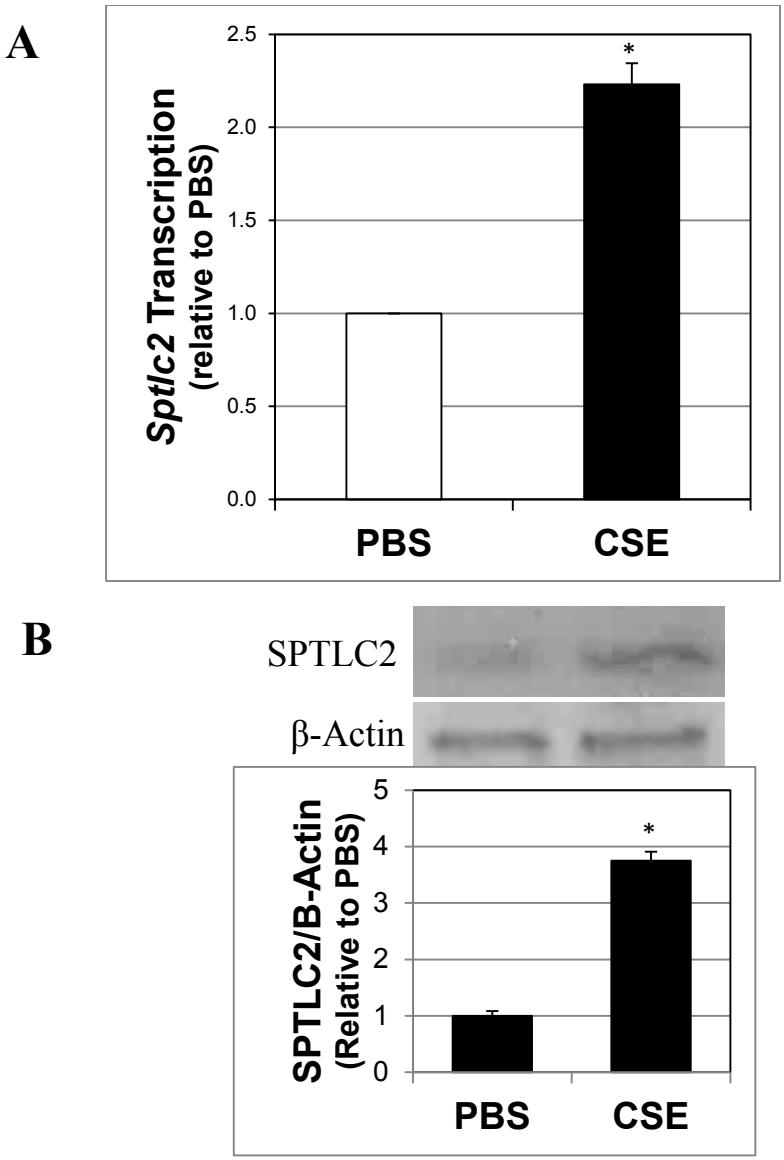

Figure 2.2: Cigarette Smoke Extract Increases Ceramide Biosynthesis.

Alveolar type 2 cells (A549) were treated with PBS or cigarette smoke extract without (CSE) or with myriocin (CSE+Myr) suspended in growth medium. Following treatment period serine palmityoltransferase 2 gene and protein levels were measured. *, $p < 0.05$ for CSE vs. other treatments.

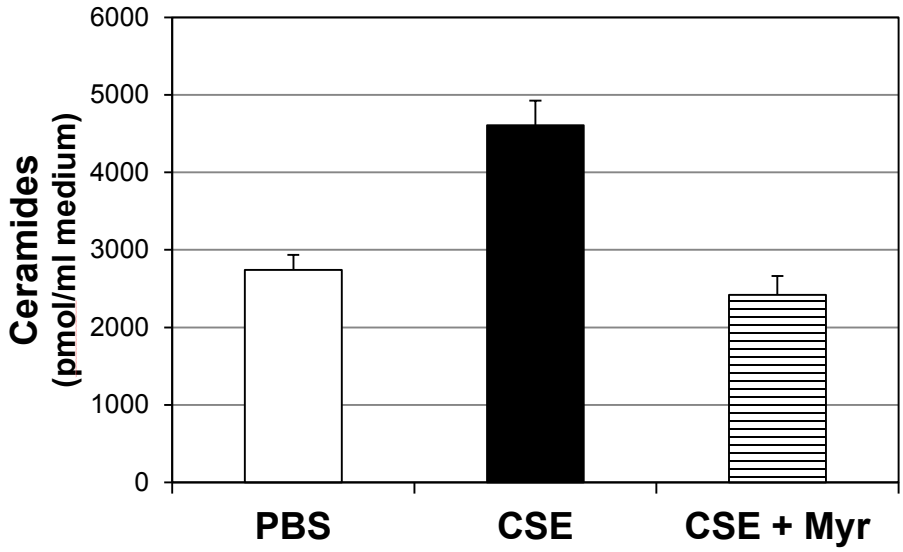

Figure 2.3: Alveolar Type 2 Cells Secrete Ceramide.

Alveolar type 2 cells (A549) were treated with PBS or cigarette smoke extract without (CSE) or with myriocin (CSE+Myr) suspended in growth medium. Following 8 h, treatment medium was replaced with fresh growth medium for 16 h, after which lipids were isolated form the medium and analyzed for ceramides. *, $p < 0.05$ for CSE vs. other treatments.

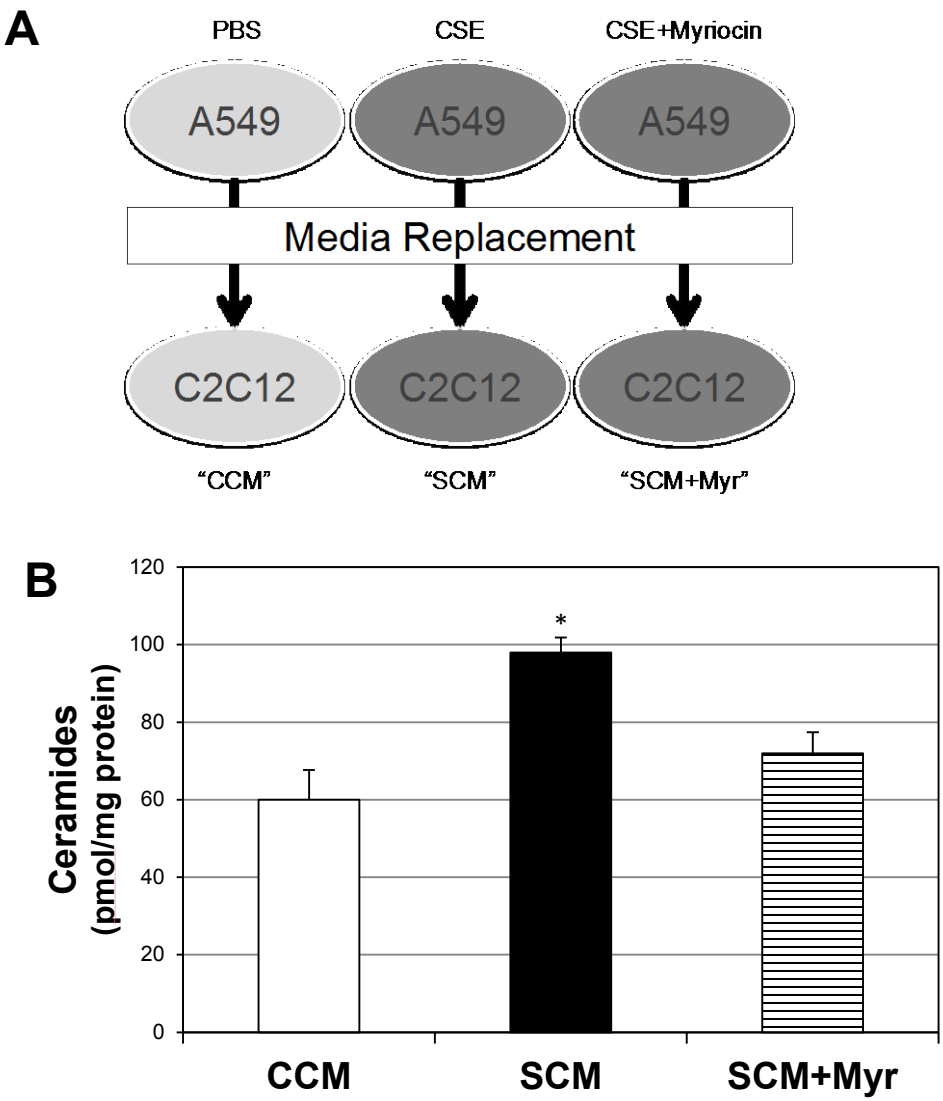

Figure 2.4: Smoke-Treated Lung Cell Conditioned Medium Increases Muscle Cell Ceramide Biosynthesis.

Skeletal muscle cells (C2C12) were treated with conditioned medium from A549 alveolar type 2 cells. A) Schematic indicating culture medium handling. B) Muscle cells treated with conditioned medium from A549 cells following incubation with control (CCM), cigarette smoke extract medium (SCM), and SCM with myriocin SCM+Myr). *, $p < 0.05$ for CSE vs. other treatments.

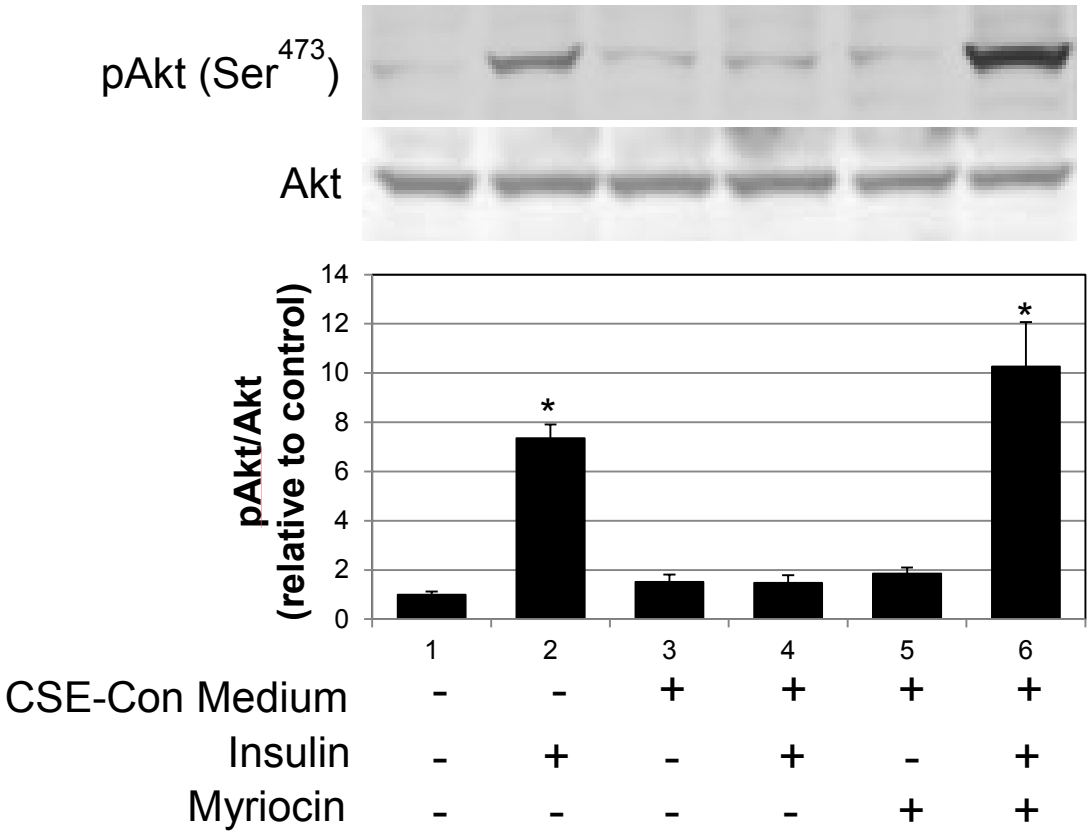

Figure 2.5: Ceramide Inhibition Prevents Lung Cell Conditioned Medium-Induced Loss of Muscle Cell Insulin Signaling.

Skeletal muscle cells (C2C12) were treated with conditioned medium from PBS- and CSE-treated A549 alveolar type 2 cells. C2C12 cells were treated with insulin following incubation with conditioned medium. C2C12 cells were treated with conditioned medium from CSE-treated A549 cells +/- myriocin to block ceramide biosynthesis.

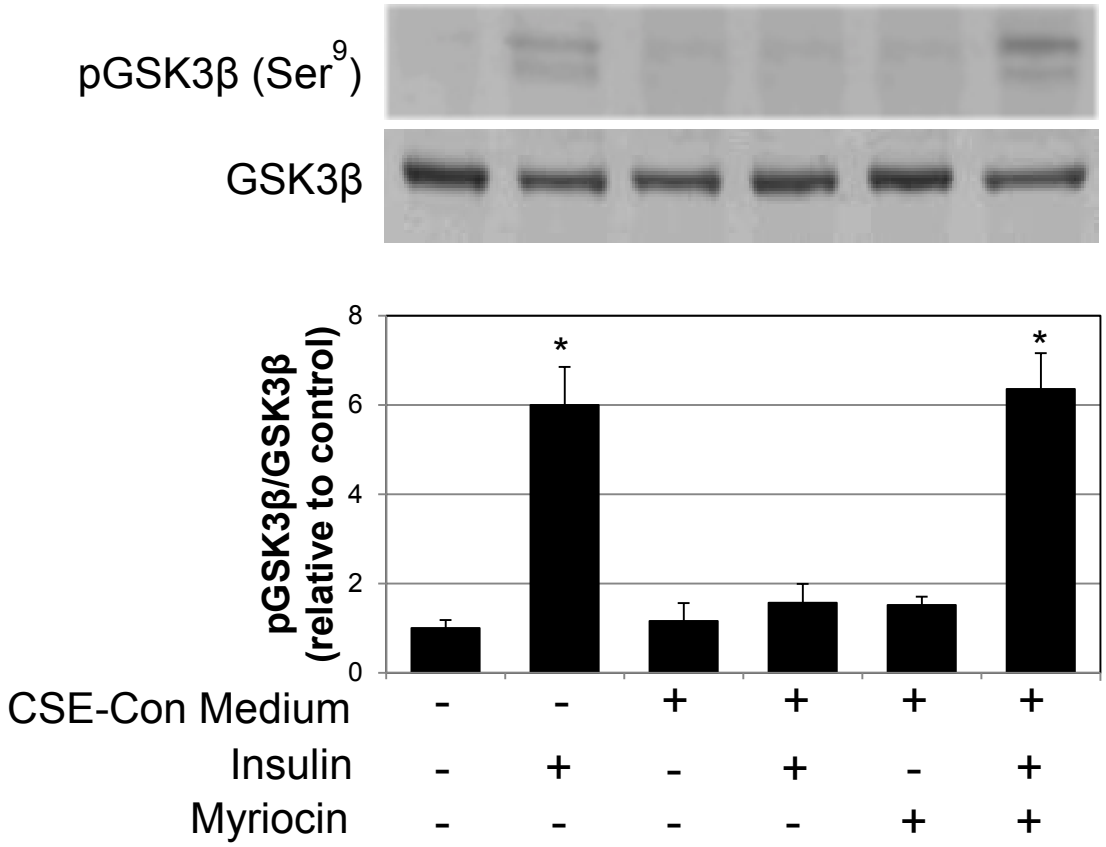

Figure 2.6: Ceramide Inhibition Prevents Lung Cell Conditioned Medium-Induced Loss Of Muscle Cell Insulin Signaling.

Skeletal muscle cells (C2C12) were treated with conditioned medium from PBS- and CSE-treated A549 alveolar type 2 cells. C2C12 cells were treated with insulin following incubation with conditioned medium. C2C12 cells were treated with conditioned medium from CSE-treated A549 cells +/- myriocin to block ceramide biosynthesis.

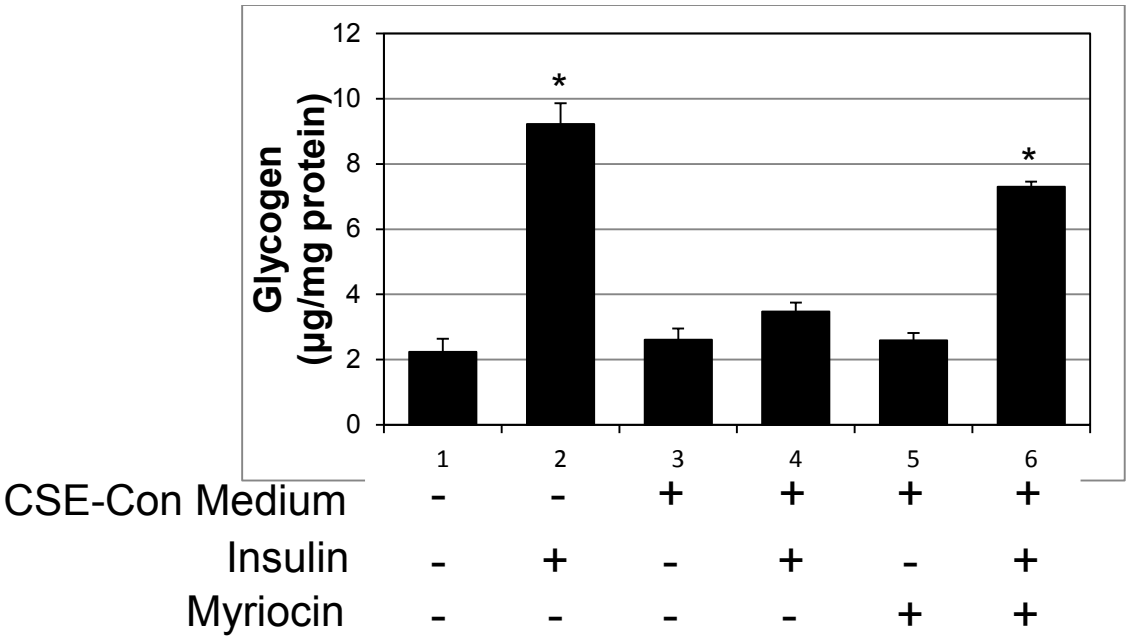

Figure 2.7: Ceramide Inhibition Prevents Lung Cell Conditioned Medium-Induced Loss Of Muscle Cell Insulin Signaling.

Skeletal muscle cells (C2C12) were treated with conditioned medium from PBS- and CSE-treated A549 alveolar type 2 cells. C2C12 cells were treated with insulin following incubation with conditioned medium. C2C12 cells were treated with conditioned medium from CSE-treated A549 cells +/- myriocin to block ceramide biosynthesis.

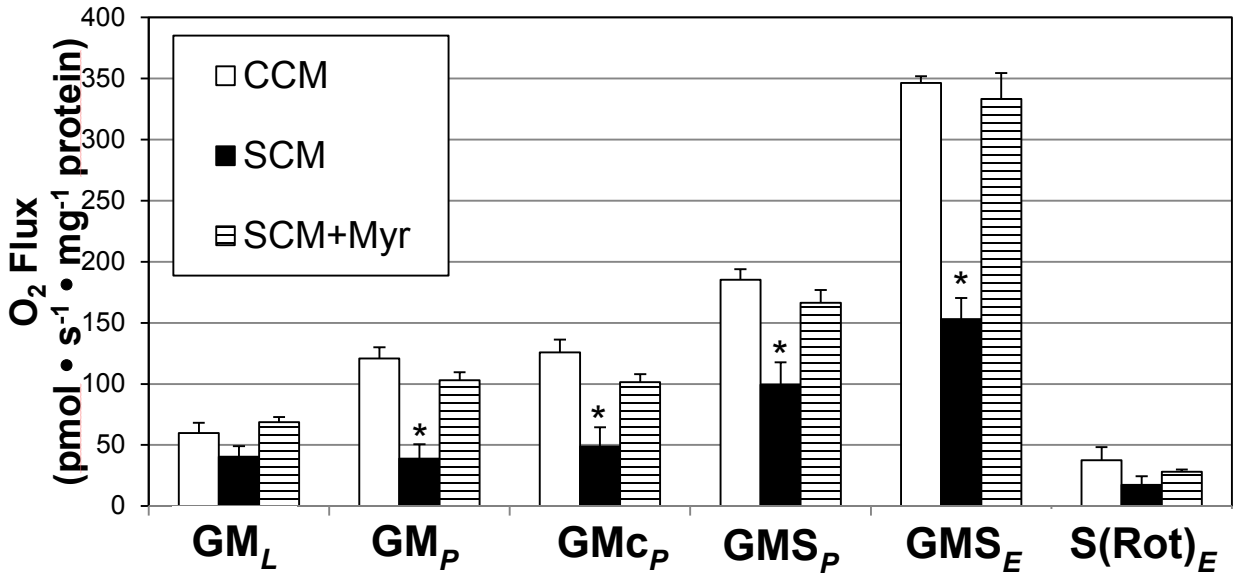

Figure 2.8: Ceramide Inhibition Protects Muscle Cell Mitochondrial Respiration.

Skeletal muscle cells (C2C12) were treated with conditioned medium from A549 alveolar type 2 cells. Myotubes were treated PBS- and CSE-A549 conditioned medium+/- myriocin (CCM, SCM, SCM+Myr, respectively). Following treatment, muscle cell mitochondrial oxygen consumption was determined according to the protocol outlined in the Methods section. *, $p <$ 0.05 for SCM vs. other treatments.

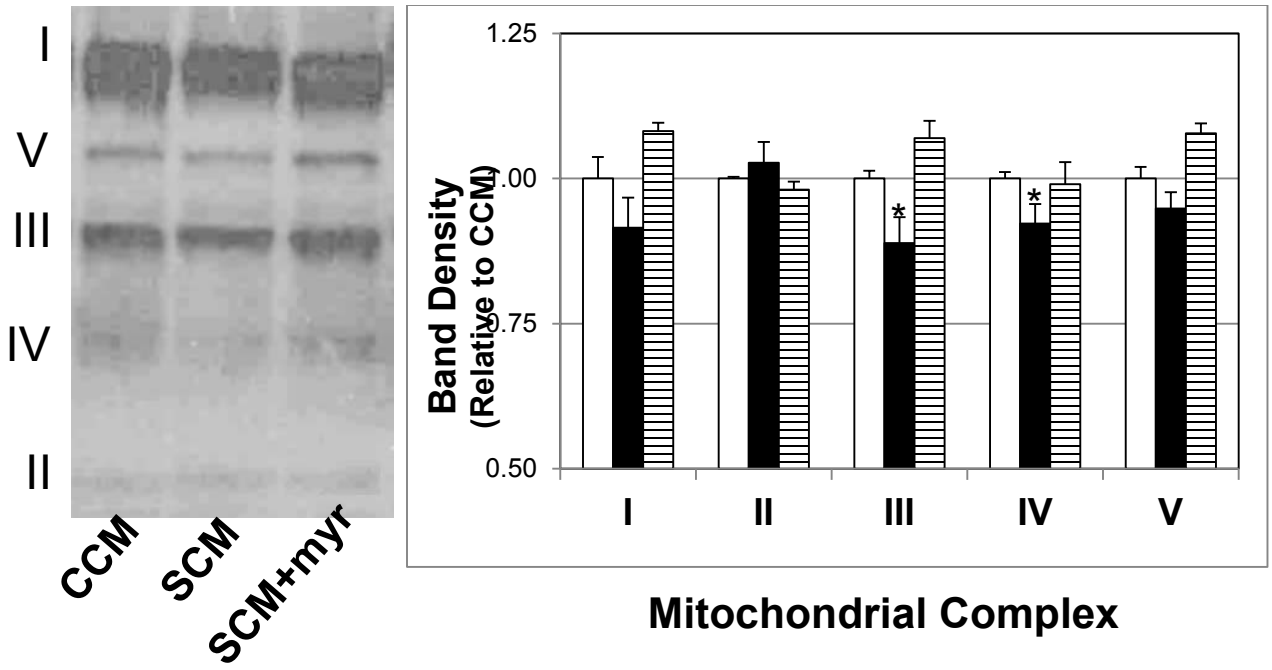

Figure 2.9: Conditioned Medium Alters Expression Of Mitochondrial Complexes III And IV, Myriocin Restores.

Skeletal muscle cells (C2C12) were treated with conditioned medium from A549 alveolar type 2 cells. Myotubes were treated PBS- and CSE-A549 conditioned medium+/- myriocin (CCM, SCM, SCM+Myr, respectively). Following treatment, mitochondrial protein levels were determined by western blot. *, $p < 0.05$ for SCM vs. other treatments.

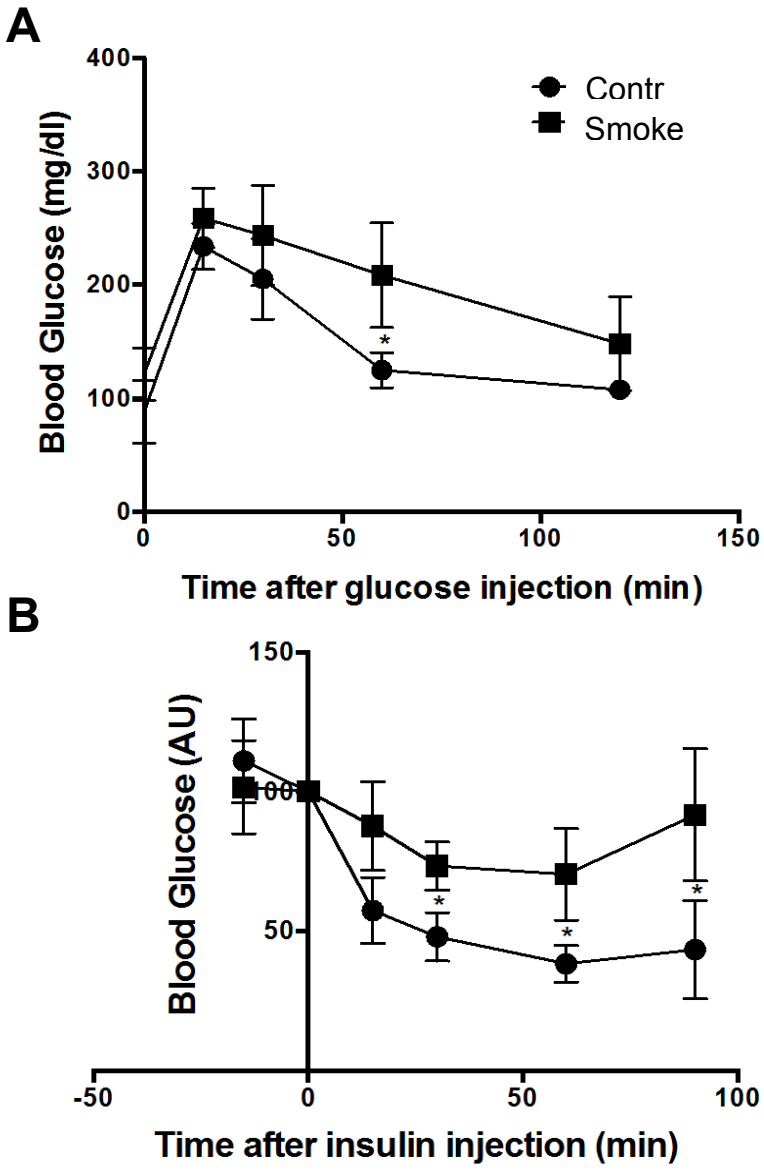

Figure 2.10: Cigarette Smoke Causes Insulin Resistance.

Adult male C57Bl6 mice were exposed to restraint (control) or side stream cigarette smoke (Smoke) daily for 6 wk. IP glucose (A; 1 g/kg BW) and insulin (B; 0.75 U/kg BW) tolerance tests were performed according to the protocol outlined in Methods.

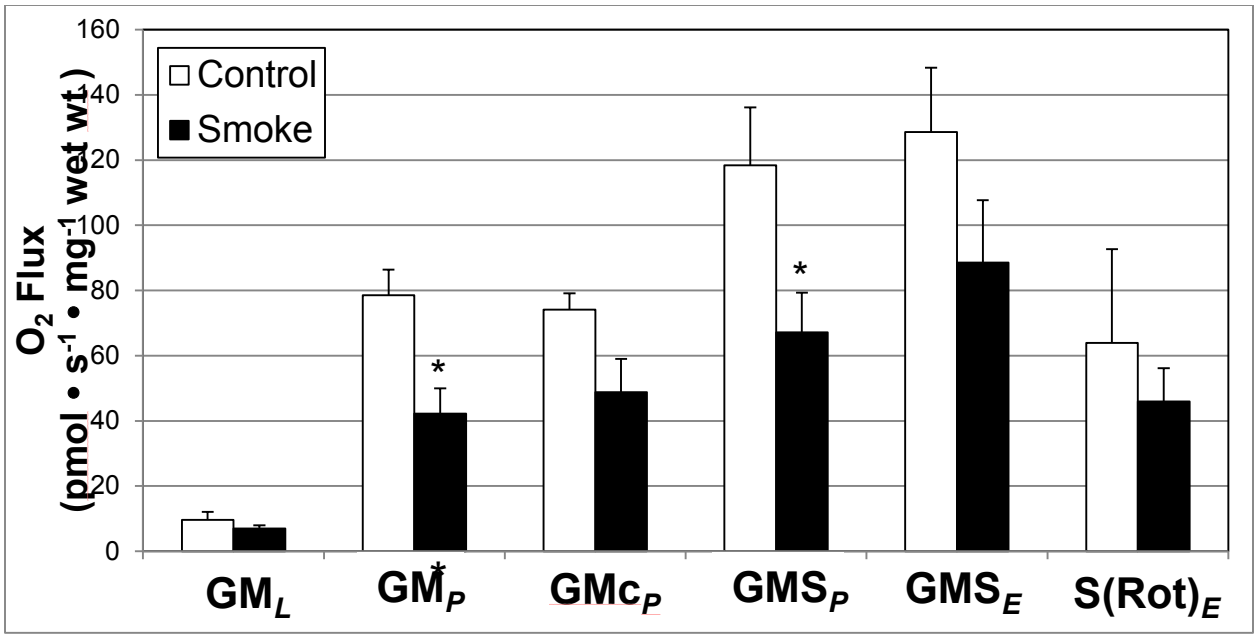

Figure 2.11: Cigarette Smoke Causes Altered Mitochondrial Respiration.

Adult male C57Bl6 mice were exposed to restraint (control) or side stream cigarette smoke (Smoke) daily for 6 wk. Mitochondrial respiration was analyzed in red gastrocnemius according to the protocol outlined in Methods.

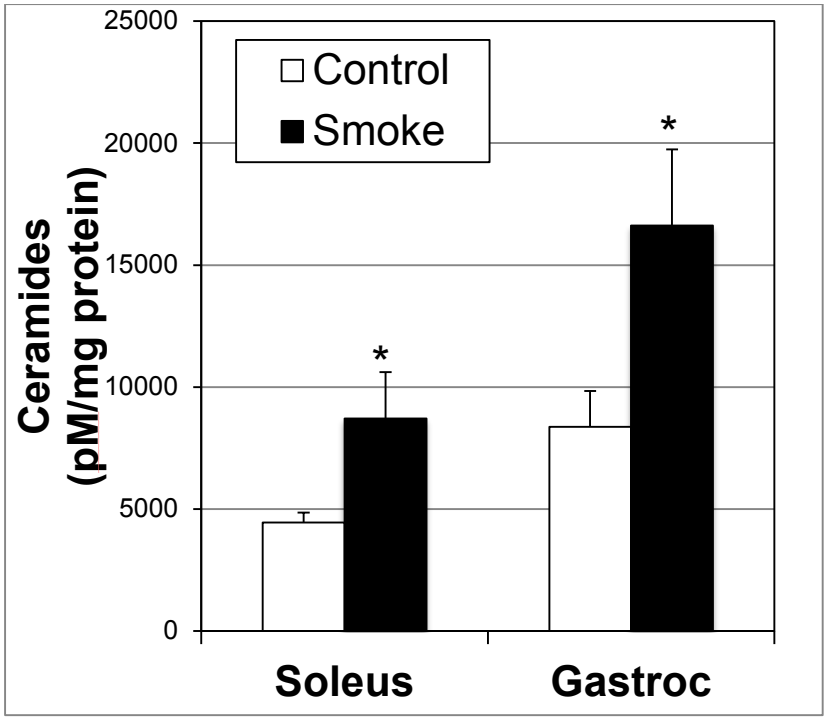

Figure 2.12: Cigarette Smoke Causes Increased Muscle Ceramides.

Adult male C57Bl6 mice were exposed to restraint (control) or side stream cigarette smoke (Smoke) daily for 6 wk. Muscles were harvested and lipids were isolated and analyzed according to the protocol outlined in Methods.

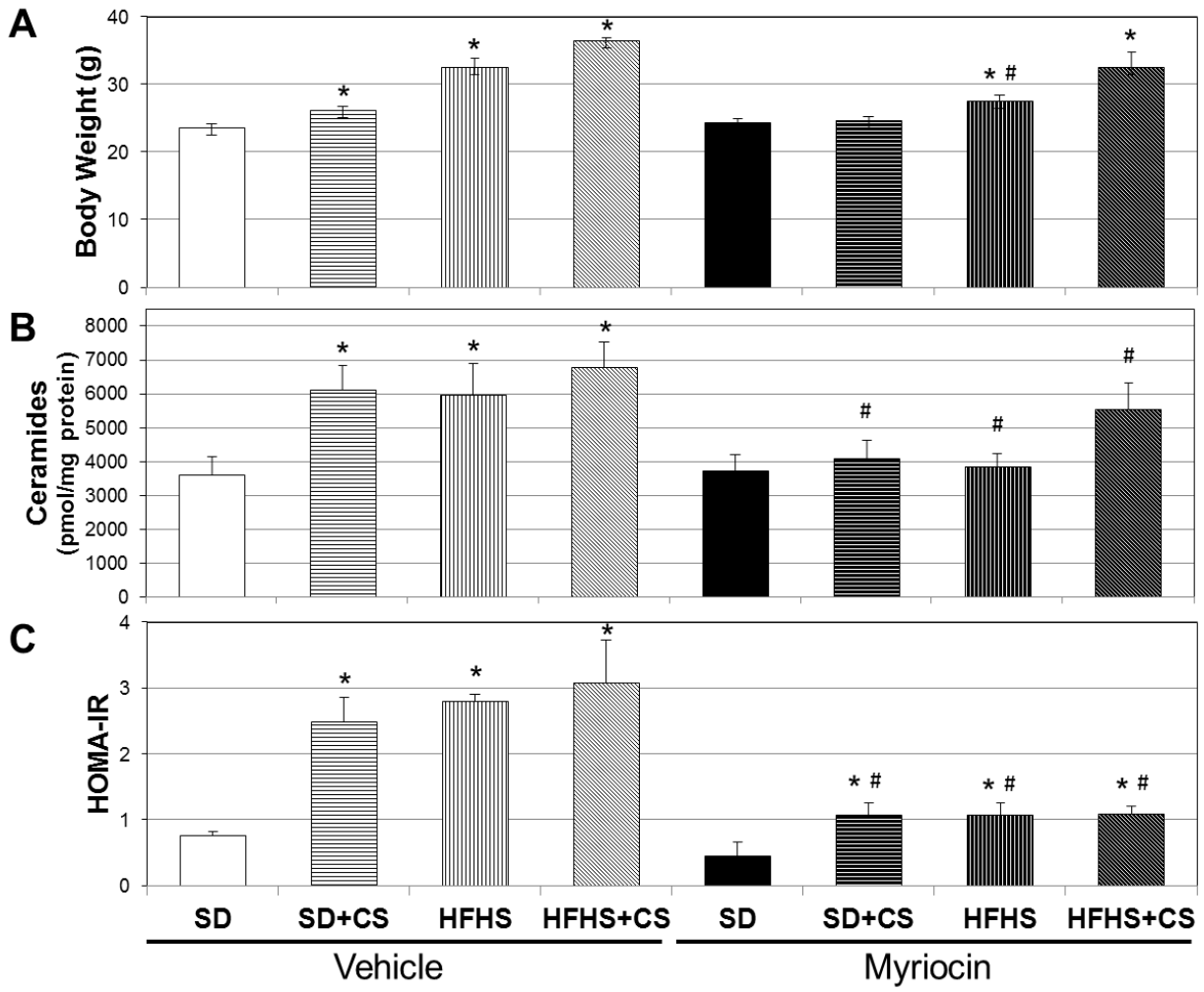

Figure 2.13: Effects Of Treatments On Metabolic Parameters.

Twelve-wk-old mice were placed on one of four treatments (SD: standard diet; SD+CS: + daily cigarette smoke exposure; HFHS: high-fat, high-sugar diet; HFHS+CS) while receiving vehicle or myriocin (0.3 mg/kg) I.P. injections every other day. Body weight (A), soleus ceramides (B), and fasting blood glucose and insulin (C) were measured in all animals at the conclusion of the study period. *, $p < 0.05$ for treatment vs. SD within each group; #, $p < 0.05$ for comparable treatment between myriocin vs. vehicle; n=6.

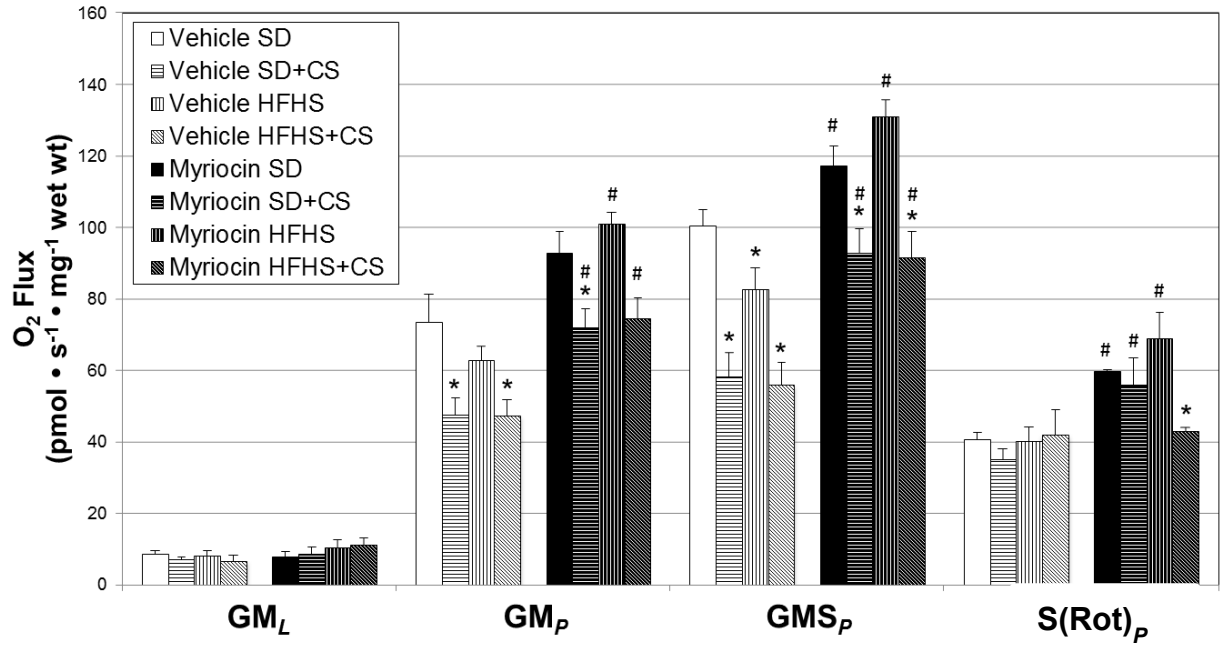

Figure 2.14: Ceramide Inhibition Protects Skeletal Muscle Mitochondrial Respiration.

Red gastrocnemius fibers were separated and permeabilized from mice following one of four treatments (SD: standard diet; SD+CS: + daily cigarette smoke exposure; HFHS: high-fat, high-sugar diet; HFHS+CS) while receiving vehicle or myriocin (0.3 mg/kg) I.P. injections every other day. *, $p < 0.05$ for treatment vs. SD within each group; #, $p < 0.05$ for comparable treatment between myriocin vs. vehicle; n=6.

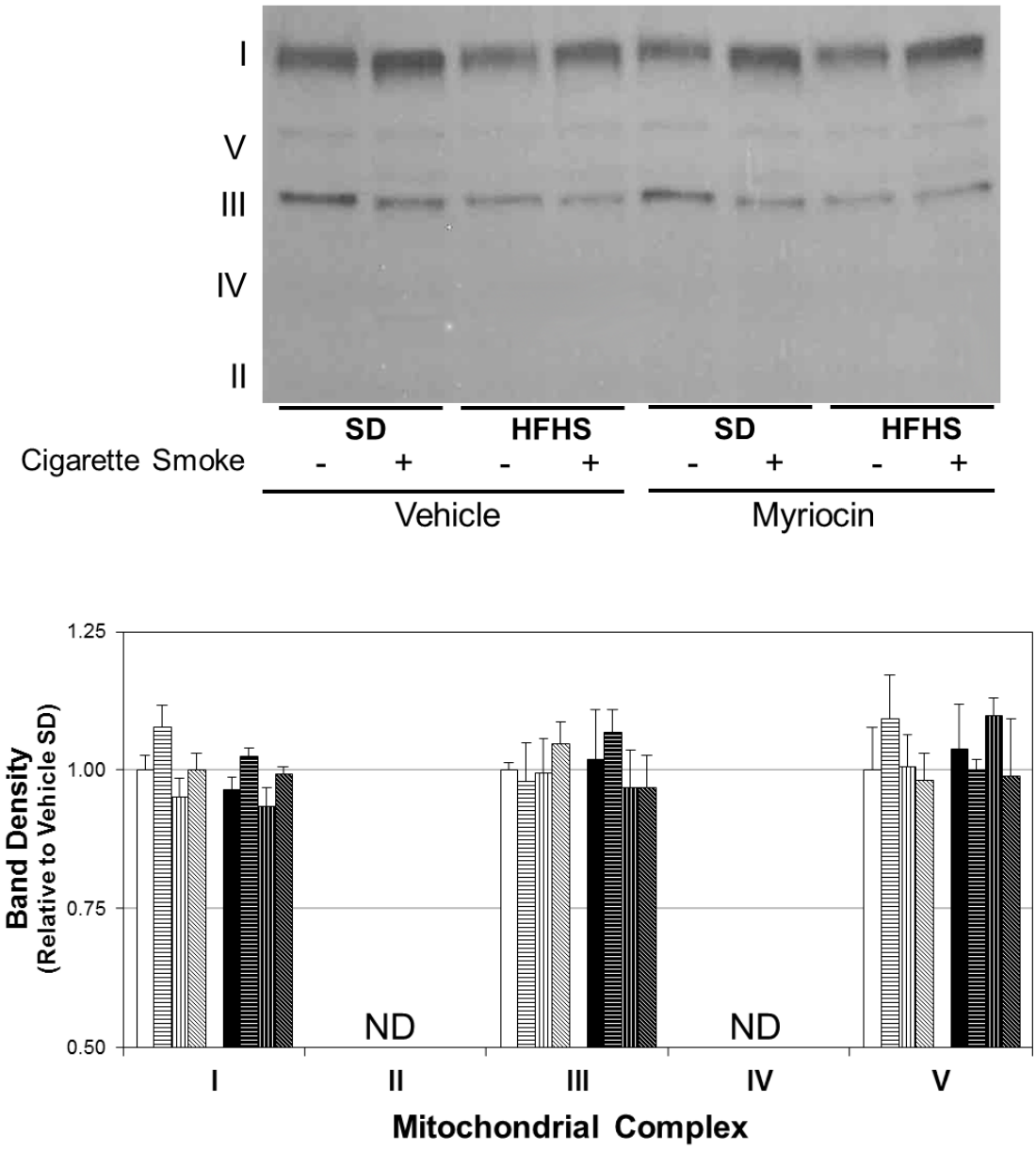

Figure 2.15: Smoking Did Not Cause Significant Differences In Mitochondrial Protein Levels.

Red gastrocnemius fibers were separated and permeabilized from mice following one of four treatments (SD: standard diet; SD+CS: + daily cigarette smoke exposure; HFHS: high-fat, high-sugar diet; HFHS+CS) while receiving vehicle or myriocin (0.3 mg/kg) I.P. injections every other day. Western blot was performed on sample lysates to determine levels of mitochondrial complexes (B; n 4).

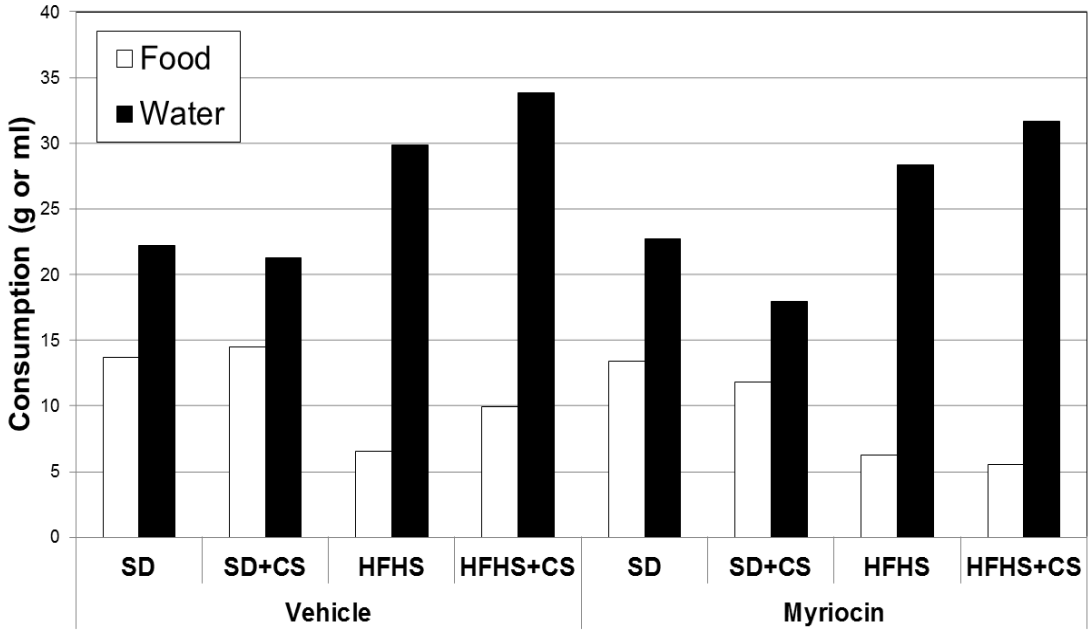

Supplemental Figure 2.1: Weekly Food And Water Consumption Does Not Vary Among Treatment Groups.

Food (g) and water (ml) consumption was measured for one week near the end of the study period. No statistically significant differences were found.

CHAPTER 3: HMGB1 as a Mediator of Cigarette Smoke-Induced Insulin Resistance

Abstract

Cigarette smoking causes inappropriate ceramide accumulation, which interferes with normal insulin signaling to cause insulin resistance. Extracellular HMGB1 is a pattern-recognition receptor ligand that is upregulated with cigarette smoke exposure, as well as metabolic alterations such as obesity. We sought to determine whether HMGB1 is a mediator of smoke-induced insulin resistance. After confirming that HMGB1 protein levels were increased in skeletal muscle with chronic cigarette smoke exposure, we found that exogenous HMGB1 interrupted normal insulin signaling *in vivo* and *in vitro*. HMGB1 increased muscle cell ceramide levels and disrupted mitochondrial function, manifested in altered respiration and increased oxidative stress, an effect that was alleviated with ceramide inhibition. However, ceramide inhibition failed to prevent HMGB1-induced reduced insulin signaling. These data suggest that HMGB1 may be a component in the metabolic disruption accompanying cigarette smoke exposure.

Introduction

Cigarette smoking causes insulin resistance, inextricably linking two of the biggest global killers. Inappropriate ceramide accumulation seems to be involved in the development of cigarette smoke-induced insulin resistance, but much of the pathway remains to be resolved (Thatcher, Tippetts et al. 2014). There is currently no ceramide-blocking therapy safe for use in humans, so clarifying the molecular mechanisms of this relationship could provide pharmaceutical targets that would reduce metabolic complications of cigarette smoking, especially for those unwillingly exposed to secondhand smoke or to smoking during gestation. It

may also be relevant in the study of the metabolic impact of pollution, since the lung responds similarly to the particulate matter of pollutants (such as diesel exhaust) and cigarette smoke.

Unlike most tissue, the lung constitutively expresses the pattern recognition receptor RAGE (receptor for advanced glycation end products) throughout adulthood and RAGE-induced inflammation has thus been an important research angle in emphysema, lung cancer, COPD, and other lung diseases (Brett, Schmidt et al. 1993; Bierhaus, Humpert et al. 2005; Reynolds, Kasteler et al. 2008; Robinson, Stogsdill et al. 2012). Advanced glycation end products (AGEs) and many non-AGE ligands bind to RAGE to activate the NF-kB, ERK1/2, JNK, and JAK/STAT pathways. In cell types that do not normally express RAGE, ligand accumulation or transcription factor activation will prompt RAGE transcription and translation during stress (Brett, Schmidt et al. 1993; Bierhaus, Humpert et al. 2005).

Interestingly, RAGE-null mice exposed to cigarette smoke do not accumulate ectopic ceramide the way wild-type mice do (unpublished, Bikman and Reynolds labs). This draws attention to the possible role of one or more RAGE ligands upstream of ceramide production in smoke-induced insulin resistance. Reynolds et al. has shown that two RAGE ligands, S100 and HMGB1, are upregulated in lung cells exposed to cigarette smoke extract (CSE)(Reynolds, Kasteler et al. 2008). HMGB1 has previously been implicated in the pathogenesis of many inflammatory diseases, including sepsis, rheumatoid arthritis, chronic kidney disease, systemic lupus erythematosis, and cancer (Musumeci, Roviello et al. 2014), all of which have also been correlated with insulin resistance in various studies. Based on these observations we sought to determine whether exogenous HMGB1 is sufficient to cause metabolic disruption following cigarette smoke exposure. If HMGB1 is involved in the etiology of insulin resistance, it may

provide an easily-accessible target for small-molecule drug interventions that could revolutionize the treatment of insulin resistance-based disease.

Materials and Methods

Cell Culture

C2C12 muscle cells were maintained in DMEM + 10% FBS. For differentiation into myotubes, myoblasts were grown to confluency and the medium was replaced with DMEM + 10% horse serum (Invitrogen, Grand Island, NY). Myotubes were used for experiments on day 4 of differentiation. Where indicated, cells were treated with myriocin (10 μM, Sigma, M1177) or rHMGB1 (20 nM) for 16 hours. Muscle cells were harvested for respiration, protein isolation, and lipid isolation following treatments.

Animals

Male C57Bl6 mice were housed in a conventional animal house and maintained on a 12-hour light–dark cycle. Two animal studies were conducted—a smoking study and an HMGB1 study. Animals received standard diet chow (Harlan Teklad 8604) and water ad libitum. For the first study, at 12-14 wk of age animals were randomly divided into room air and cigarette smoke (CS)-exposed groups. Mice were placed in soft restraints and connected to the exposure tower of a nose-only exposure system (InExpose System, Scireq, Canada). Animals were nasally exposed to mainstream CS generated by research cigarettes where a computer-controlled puff was generated every minute, leading to 10 s of CS exposure followed by 50 s of fresh air. The CS-exposed group inhaled CS from two consecutive cigarettes per day for three weeks, at which point the dosage was increased to two cigarettes twice daily. Control animals were similarly

handled and restrained in fresh air for the same duration. Protein was isolated from harvested gastrocnemius and HMGB1 assayed by western blot.

For the second study, at 12-14 wk of age animals were randomly divided into a control and treatment group and received daily i.p. injections of HMGB1 (1μg/day) for 2 weeks. After the 2-week course, mice underwent i.p. glucose (G7021; Sigma-Aldrich, St. Louis, MO) and insulin (Actrapid; Novo Nordisk, Plainsboro, NJ) tolerance tests. For both tests, mice were fasted for 10 hours and received an injection of either glucose (1 g/kg body weight) or insulin (0.75 U/kg body weight). Blood glucose was determined at the times indicated in the figures, using the Bayer Contour glucose meter. Tissues were harvested at the conclusion of the study period. Studies were conducted in accordance with the principles and procedures outlined in the National Institutes of Health Guide for the Care and Use of Laboratory Animals and were approved by the Institutional Animal Care and Use Committee (IACUC) at Brigham Young University.

Lipid Analysis

For ceramide specific lipid isolation, homogenized tissues were re-suspended in 300 μl ice-cold PBS and 1.5 mL of methanol. 500 pmol of internal C-17 ceramide (Avanti Lipids; 860647) standard was spiked into each sample. Samples were centrifuged and supernatant was transferred to a clean tube. Following the addition of 30 μl of 1 M KOH in methanol, samples were incubated overnight at 50°C. Samples were dried to 50% volume and 25 μl glacial acetic acid was added to neutralize KOH. Separation of aqueous and organic phases required addition of 300 μl LC-grade chloroform and 600 μl DDH2O followed by centrifugation for 2 minutes at maximum speed. The lower organic phase was transferred to a fresh vial. This separation step

was repeated twice. All lipid samples were dried in a vacuum centrifuge (Eppendorf Concentrator Plus).

Lipids were characterized and quantified using a shotgun lipidomics technique on a Thermo Scientific LTQ Orbitrap XL mass spectrometer. Evaporated lipid samples were re-suspended in a 2:1 chloroform: methanol Folch solution (200 μL). The re-suspended lipids were then combined with a modified 2:1:1.25 chloroform: methanol: isopropanol Bligh and Dyer solution (800 μL) with 15 mM ammonium acetate acting as an ionizing adduct. A 1.74 μM phosphatidylethanolamine internal standard (1 μL) was spiked into each sample for mass calibration and characterization data alignment. Samples were analyzed using a 2.5-minute mass-window scanning method in positive-ion mode at a resolution of 60,000 (fwhm at 400 mz) for all primary MS1 scans. MS2 fragmentation data was also collected and manually verified for each mass window to give additional confidence to the correct identification of abundant lipid species. Three technical replicate mass spectrometer runs were performed on each sample. Samples were injected at 10 μL/min using a direct-inject electrospray ionization (ESI) soft-ionization spray head from a Hamilton GASTIGHT glass syringe. The spray voltage and capillary temperature were maintained at 5.0 KV and 275oC respectively. Each technical replicate was run in random order to reduce systematic bias. Data were analyzed using in-house developed peak summarization, recalibration, and lipid identification software using lipid database information from the LIPID Metabolites and Pathways Strategy (Lipid MAPS) Lipidomics Gateway database (Fahy, Subramaniam et al. 2009). To ensure high-confidence identifications, an intensity threshold estimated to be 5% above instrumental static signal was implemented. Lipid identities were only assigned when significantly observable peaks were identified in at least two of the three technical replicate runs. Non-zero lipid quantities were averaged from the replicate runs.

The lipid species identified across different ionization states or with adducts were totaled together. Quantification was completed by normalizing total ion counts to the relative abundance of the internal standard that was spiked into each sample.

Cell and Muscle Fiber Bundle Permeabilization

For cells, C2C12 myotubes were scraped from culture dishes with mitochondrial respiration buffer 05 (MiR05; 0.5 mM EGTA, 10 mM KH2PO4, 3 mM MgCl2-6 H2O, 60 mM K-lactobionate, 20 mM HEPES, 110 mM Sucrose, 1 mg/ml fatty acid free BSA, pH 7.1). Contents were transferred to a tube and centrifuged for 10 min at 1000 rpm at RT. After removal of supernatant, cells were resuspended in MiR05 plus 1 mg/ml digitonin and gently rocked at RT for 5 min before centrifugation at 1000 rpm for 5 min. After discarding supernatant, cells were then suspended in 2.2 ml warm MiR05 and transferred to chambers in the O2K (Oroboros Instruments). Following respiration protocol (outlined below), cells were removed from the chambers and used for further analysis, including protein quantification.

For skeletal muscle, red gastrocnemius was quickly removed from mice following cervical dislocation and immediately placed in ice-cold MiR05 and trimmed of connective tissue. Small fiber bundles were prepared and gently separated along their longitudinal axis to a size of 5-25 mg. Bundles were then transferred to a tube with chilled MiR05 and 50 µg/ml saponin and rocked at 4˚C for 30 min, then washed in MiR05 at 4˚C for at least 15 minutes.

Mitochondrial Respiration Protocol

High-resolution O2 consumption was determined at 37˚C in permeabilized cells and fiber bundles using the Oroboros O2K Oxygraph (Innsbruck, Austria) with MiR05 respiration buffer as described previously (38, 47). Respiration was determined by all or parts of the following substrate-uncoupler-inhibitor-titration (SUIT) protocol (32): electron flow through complex I

was supported by glutamate+malate (10 and 2 mM, respectively) to determine oxygen consumption from proton leak (GML). Following stabilization, ADP (2.5 mM) was added to determine oxidative phosphorylation capacity (GMP). Where indicated, outer mitochondrial membrane integrity was tested by adding cytochrome c (10μM; GMcP). Succinate was added (GMSP) for complex I+II electron flow into the Q-junction. To determine full electron transport system (ETS) capacity over oxidative phosphorylation in cells, the chemical uncoupler carbonyl cyanide 4-(trifluoromethoxy) phenylhydrazone (FCCP) was added (0.05 μM, followed by 0.025 μM steps until maximal O2 flux was reached). Complex II-supported ETS was then measured by inhibiting complex I with rotenone (Rot; 0.5 μM). Lastly, residual oxygen consumption was measured by adding antimycin A (2.5 μM) to block complex III action, effectively stopping any electron flow. This value provides a rate of respiration that is used as a baseline.

Statistics

Data are presented as the mean ± SEM. Data were compared by ANOVA with Tukey's post-hoc analysis (Graphpad Prism; La Jolla, CA). Significance was set at $p<.05$.

Results

Smoking Increases HMGB1 Levels in Mouse Gastrocnemius

Previous work in the Reynolds lab showed that two RAGE ligands—HMGB1 and S100—are increased in cultured lung cells after exposure to cigarette smoke extract (CSE) (Reynolds, Kasteler et al. 2008). These results had yet to be confirmed *in vivo* and, as far as we know, we are the first to investigate any role for HMGB1 in skeletal muscle. After 8 weeks of daily cigarette smoke exposure, HMGB1 was upregulated in mouse gastrocnemius as compared to unexposed controls (Fig. 3.1).

Exogenous HMGB is Sufficient to Induce Insulin Resistance

CSE exposure decreases pAkt in C2C12s after insulin stimulation (Fig. 2.5) and we sought to determine whether HMGB1 caused the same interruption in insulin signaling as proof of concept before working in a mouse model. We found that insulin stimulation expectedly increased pAKT more in control and myriocin-treated cells, and that this was mitigated with HMGB-1 treatments. Unexpectedly, ceramide inhibition with myriocin failed to protect insulin signaling in the presence of HMGB1 (Fig. 3.2). We found HMGB1 was capable of similar results in mice. After two weeks of daily injections, HMGB1-injected mice were significantly less glucose tolerant and less insulin sensitive than their vehicle-injected counterparts (Fig. 3.7).

After two weeks of daily injections, HMGB1 mice exhibited different glucose and insulin tolerances than their vehicle-injected counterparts (Fig. 3.3). Thirty minutes into the glucose tolerance test, the mean blood glucose of the vehicle control group was 206 mg/dL (SD=38, n=6) while the HMGB1 group had reached 344 mg/dL (SD=86, n=4) and the disparity continued through the end of the time course. When injected with insulin, the vehicle-treated mice had a mean blood sugar of 72 mg/dL at 30 minutes (SD=10, n=6), while the HMGB1 mean was 112 mg/dL (SD=4, n=6).

Ceramide accumulation is a mechanism of insulin resistance in smoke-induced and diet-induced models, and HMGB1 appears to cause the same dramatic upregulation of ceramide synthesis. HMGB1 treatment increased ceramide in cultured myotubes four-fold (Fig. 3.4), while myriocin performed its expected role in halting ceramide synthesis.

HMGB1 Alters Mitochondrial Function in Skeletal Muscle

C2C12 myotubes were treated with 20 nm HMGB1 with or without myriocin for 16 hours before being permeabilized to measure cellular respiration in a substrate-uncoupler-

inhibitor titration protocol. HMGB1 had a dampening effect on mitochondrial respiration in myotubes (Fig. 3.5) while increasing oxidative stress (Fig. 3.6), though no apparent effect on levels of mitochondrial complex proteins. Interestingly, ceramide inhibition tended to protect mitochondrial function in spite of HMGB1 treatment (Fig. 3.5).

A dichlorofluorescein assay (Fig. 3.6) revealed that while the regular HMGB1 dose had no effect, a high dose (5x regular concentration) of HMGB1 increased oxidative stress in myotubes. Myriocin treatment brought the oxidative stress back down, significantly lower than HMGB1 alone.

Discussion

The primary conclusion of this study is that HMGB1 is sufficient to cause insulin insensitivity in cultured C2C12s and *in vivo.* Given the many disease states that exhibit elevated HMGB1, including lupus, rheumatoid arthritis, and sepsis, this conclusion invites investigation into its potential roles in various etiologies. This is especially true in the case of cigarette smoke-induced metabolic disruption: smoking does increase HMGB1 expression and HMGB1 can itself cause insulin resistance. While RAGE-ligand interactions are broadly considered responsible for the nerve and blood vessel damage of late diabetic complications, we are the first to implicate it in the development of pre-diabetes.

The question of whether HMGB1 impacts other aspects of cellular metabolism remains unanswered. The possible restoration of normal respiration in HMGB1-treated cells or muscle with myriocin treatment suggests that HMGB1 does have an impact and is of interest because it would place HMGB1 and ceramide on the same continuum: HMGB1 increases and activates RAGE and TLR 4, leading in term to ectopic ceramide accrual.

The upregulation of the SPT2 gene transcript does suggest extra ceramide production and the shift in the drp1/mfn likely reflects a shift in mitochondrial dynamics toward greater fission, which has been shown to be a consequence of excess ceramides. However, ceramide in myotubes is much more clearly elevated than in whole muscle and, again, this leaves us with something of a paradox. Prior work has shown that blocking mitochondrial fission completely restores normal respiration in the presence of ceramide, so it appears that fission is an essential component of ceramide-induced disruption of respiration (Smith, Tippetts et al. 2013). Thus, we plan to use mdivi-1 to block mitochondrial fission in C2C12s and treat with HMGB1 as another way to gauge ceramide's involvement in HMGB1-induced disruption. We are interested in whether looking at individual ceramide species would reveal clearer trends in skeletal muscle response to HMGB1, but acknowledge the risk of data-mining. We will certainly use RNA from gastroc samples to see whether the SPT2 transcript was upregulated.

HMGB1 is found in the nuclei of almost all mammalian cells, serving a peaceful role as a non-histone DNA-binding protein. Extracellularly, it serves as a pro-inflammatory cytokine and thus is normally studied in plasma, sputum, or other secretions. We are the first to observe its increased expression in skeletal muscle. HMGB1 is also known to accumulate in the cytoplasm before being secreted by cells under duress, but since our western blot may simply have captured the HMGB1 present in the blood vessels and extracellular spaces of the gastroc, determining HMGB1 localization is vital follow-up. We plan to stimulate C2C12s with cigarette smoke extract and differentially measure HMGB1 in the cells and secreted into the cell medium. Additionally, we hope to obtain a clearer western blot.

So far, we do not know HMGB1's inflammatory actions were mediated through the activation of RAGE, TLRs, or other receptors. RAGE is a unique pattern recognition receptor in

that it binds mainly to endogenous compounds. HMGB1 is known mostly as a RAGE ligand. However, HMGB1 and HMGB1complexes with other molecules (LPS, DNA, etc.) can activate a variety of receptors whose ensuing inflammatory pathways converge. Since RAGE knock-outs exposed to cigarette smoke are spared ceramide accumulation (Bikman lab, unpublished) and TLR4 has been shown to be required for lipid-induced insulin resistance (Holland, Bikman et al. 2011), it is likely that HMGB1 works through both. We will perform a co-immunoprecipitation assay of HMGB1 with both RAGE and TLR4 in gastrocnemius to see whether either or both interactions could be implicated in HMGB1's actions. *In vitro*, it would be interesting to assess the impact of a knock-down of RAGE, TLR4, and both.

While this study began with the observation that HMGB1 is a RAGE ligand upregulated in cigarette smoking, the discovery that HMGB1—at a low dose for as little as two weeks—is sufficient to induce insulin resistance has implications far beyond smoking research. Recent work has connected diesel particulate matter to increased RAGE expression and activation (Barton, Betteridge et al. 2014); RAGE ligands are upregulated in preeclamptic placentas(Naruse, Sado et al. 2012); hyperinsulinemia in women with polycystic ovarian syndrome causes increased apoptosis via increased HMGB1 (Ni, Sun et al. 2015). Increased plasma HMGB1 has been measured in patients with a variety of insulin-resistance-related illnesses and if HMGB1 is a cause rather than only a consequence of insulin resistance it provides an attractive potential treatment target.

As connections solidify between smoking and pollution, inflammation and insulin resistance, insulin resistance and other disease, etc., HMGB1 may become a prime intervention point for a variety of conditions. Its place late in inflammation makes it uniquely accessible to

control and a variety of small molecules have already been shown to effectively inhibit it, improving inflammatory conditions (Musumeci, Roviello et al. 2014).

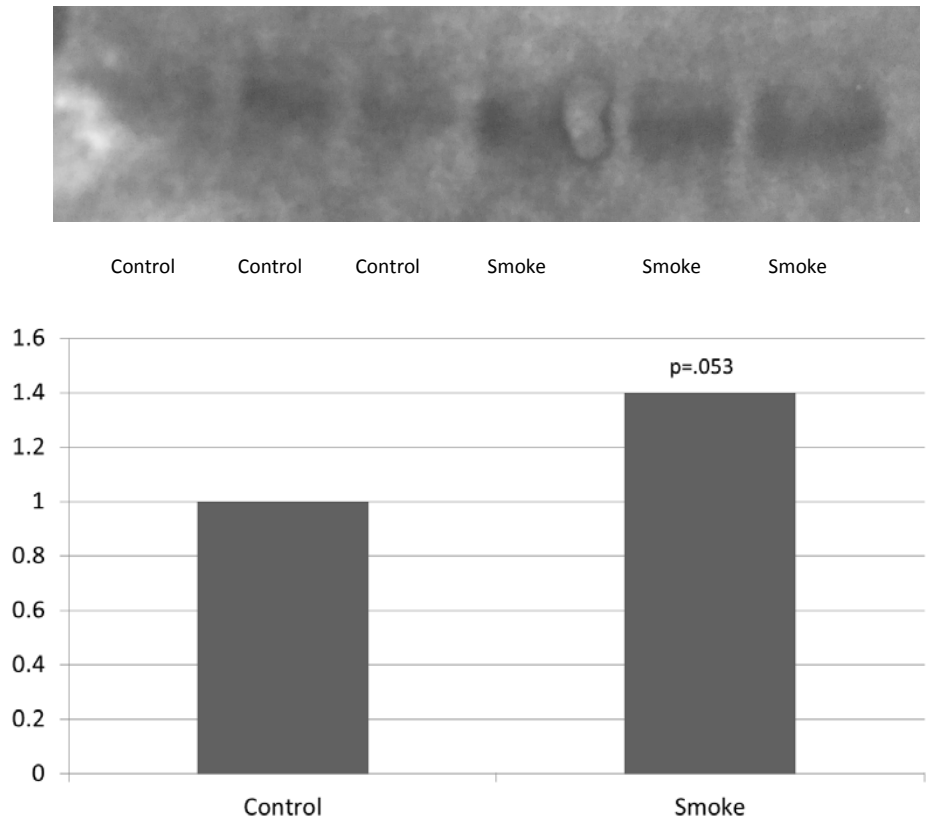

Figure 3.1: Smoking Increases HMGB1 Expression In Mouse Gastrocnemius.

Adult male mice were exposed to cigarette smoke daily for 8 weeks. Tissue was harvested and proteins quantified via western blot.

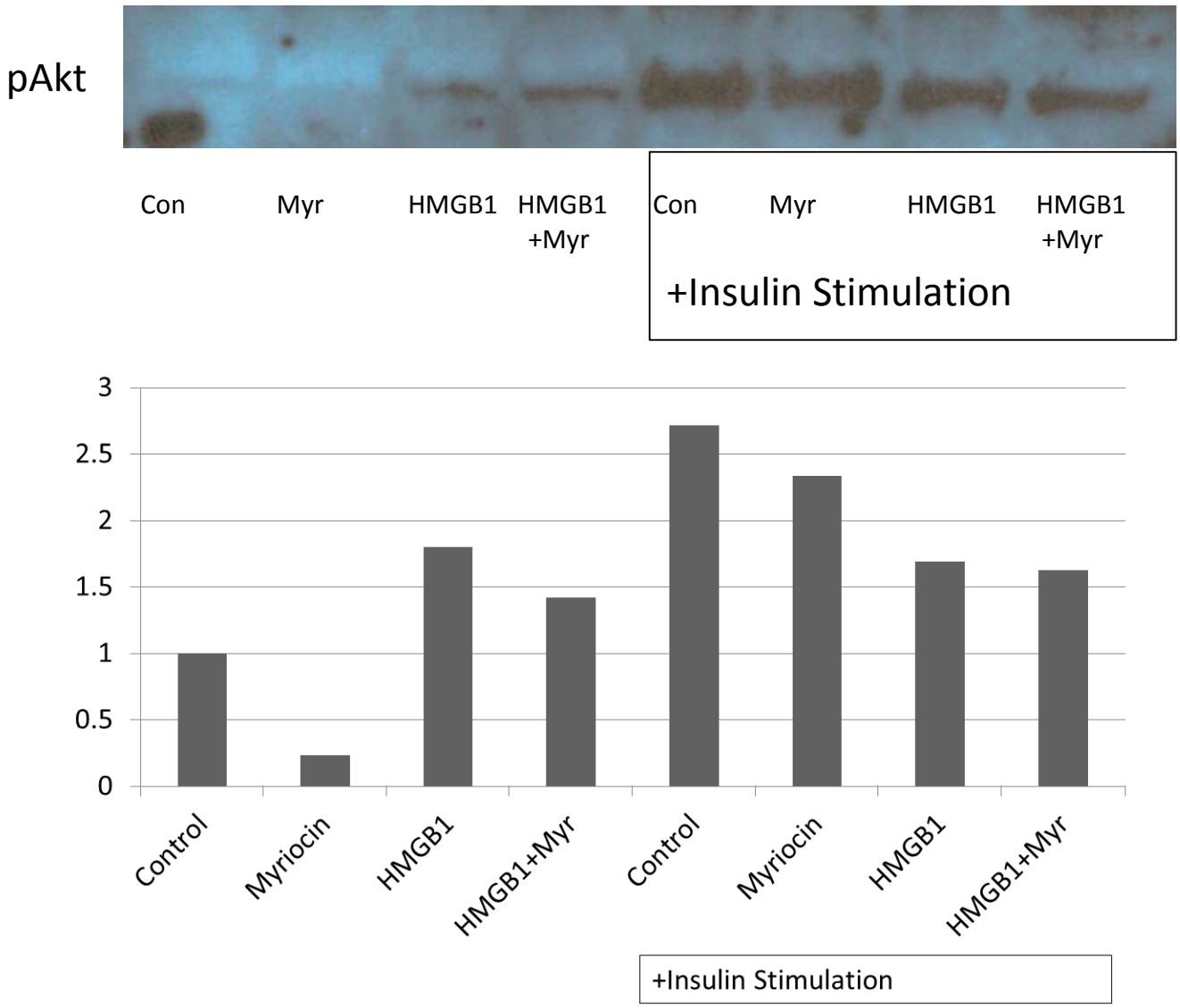

Figure 3.2: HMGB1 Impairs Akt Phosphorylation In Response To Insulin Stimulus In Cultured Myotubes.

C2C12s were grown to confluence and treated with HMGB1 and/or myriocin for 16 hours. They were then stimulated with 100 nm insulin for 10 minutes and harvested.

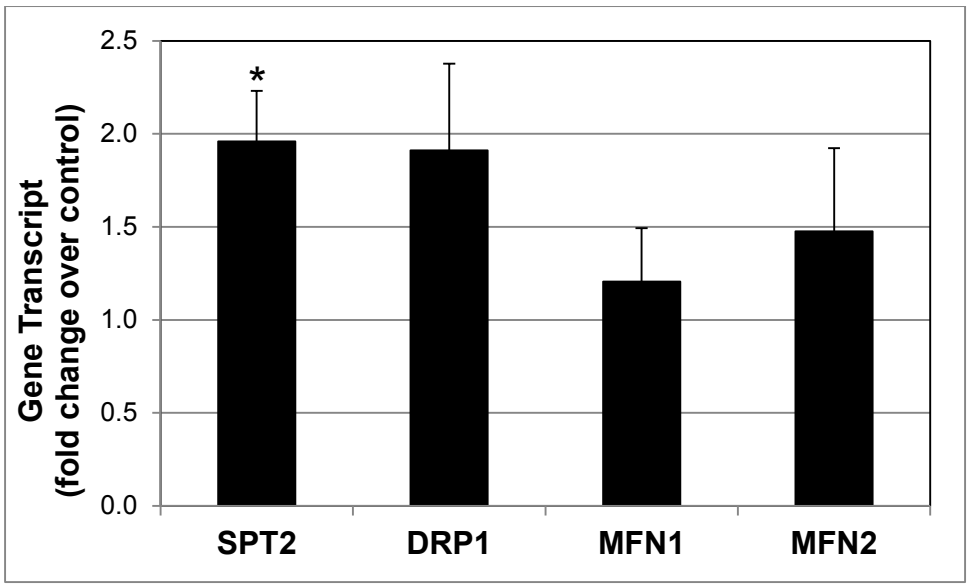

Figure 3.3: HMGB1 Upregulates Markers Of Mitochondrial Fission And Ceramide Production.

RNA was isolated from gastrocnemius of HMGB1 and vehicle-injected mice and used for reverse transcriptase and qPCR. Data were analyzed according to the protocol by Pfaffl (Pfaffl 2001).

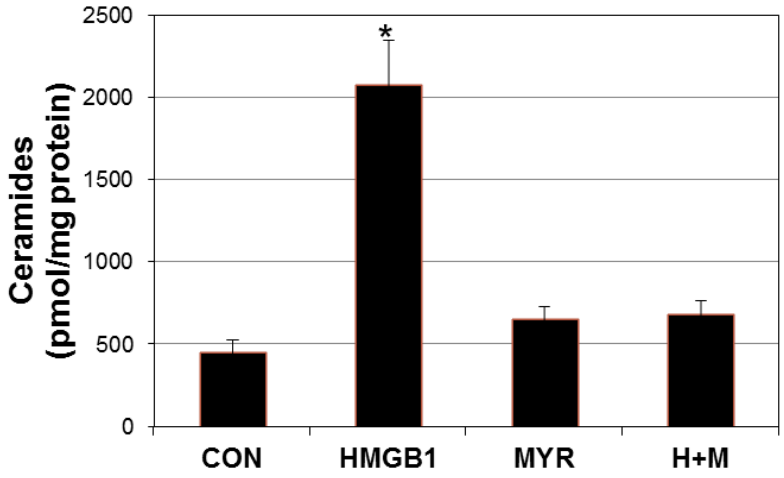

Figure 3.4: HMGB1 Increases Ceramides In Cultured Myotubes.

C2C12s were grown to confluence and treated with HMGB1 and/or myriocin for 16 hours. Lipids were harvested and analyzed as described in methods.

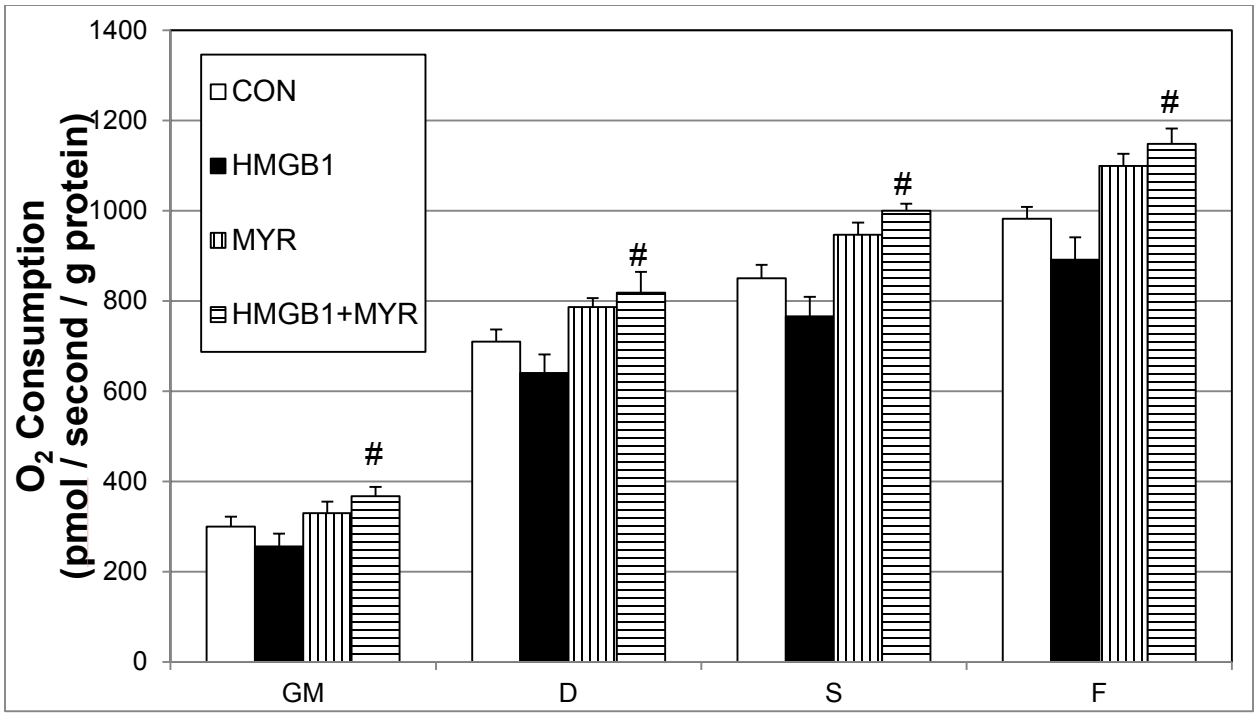

Figure 3.5: Myriocin Counters Impaired Respiration In HMGB1-Treated Cells.

O2 consumption was measured in differentiated C2C12 myotubes. The visible decrease in respiration with HMGB1 treatment is not significant, but # represents an HMGB1+Myriocin respiration that is higher than HMGB1 alone.

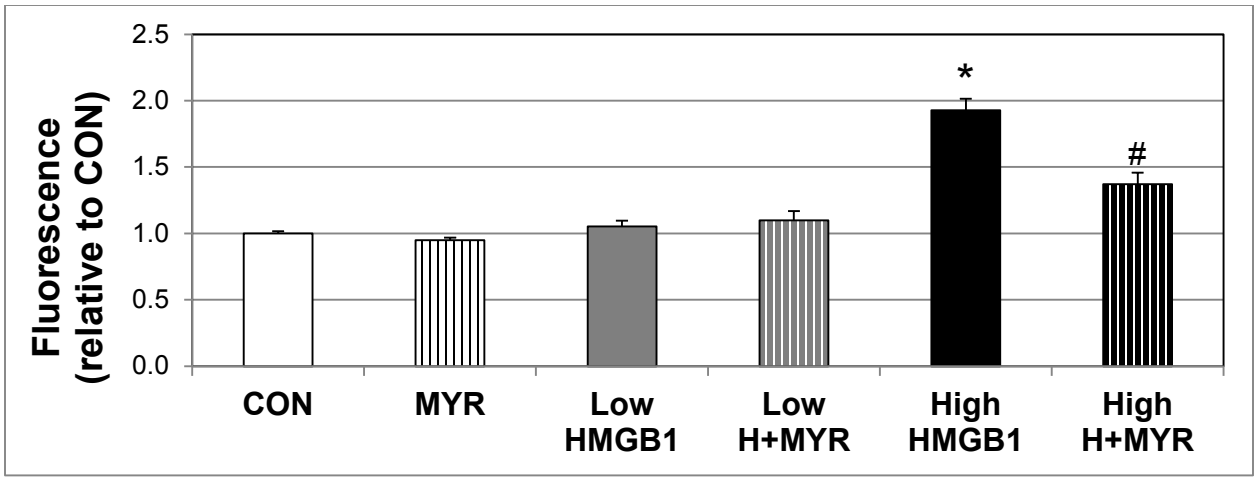

Figure 3.6: HMGB1 Causes Oxidative Stress In Skeletal Muscle Cells In A Dose-Dependent Manner.

After 16 hours of treatment with HMGB1 (high or low dose) and/or myriocin, differentiated myotubes were treated with dichlorofluorescein. Fluorescence represents oxidation levels and is a measure of cellular oxidative stress.

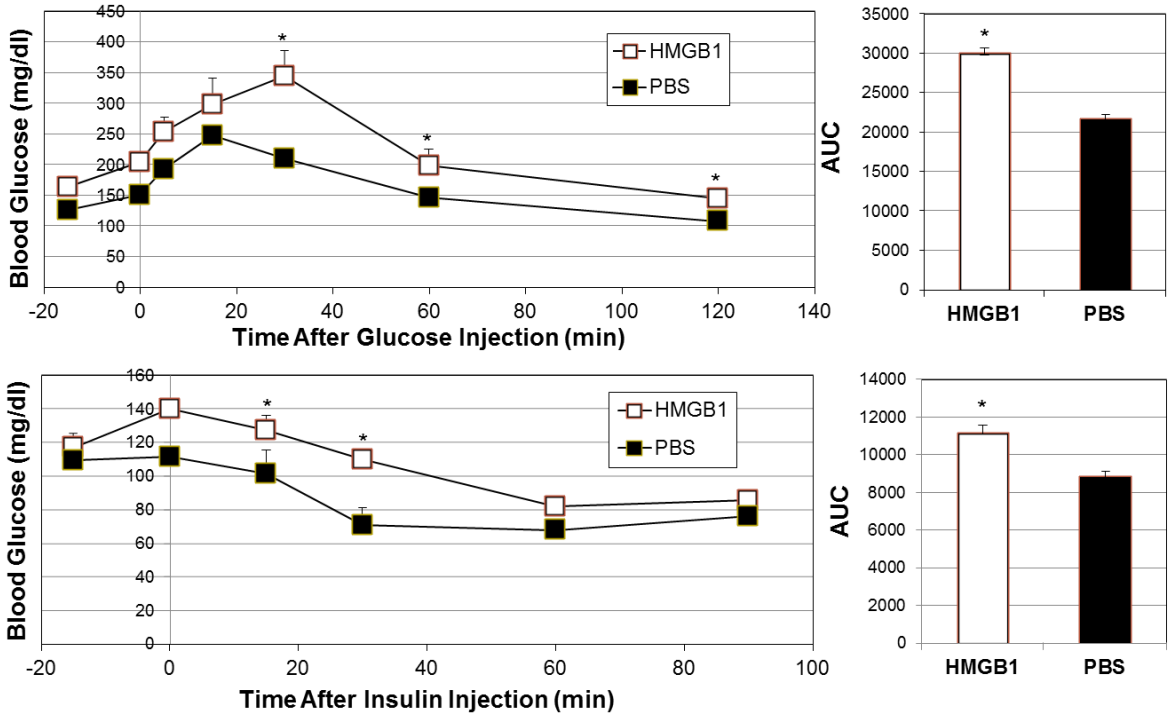

Figure 3.7: Exogenous HMGB1 Causes Insulin Resistance In Vivo.

IP glucose (A; 1 g/kg BW) and insulin (B; 0.75 U/kg BW) tolerance tests were performed on vehicle- and HMGB1-injected mice according to the protocol outlined in Methods.

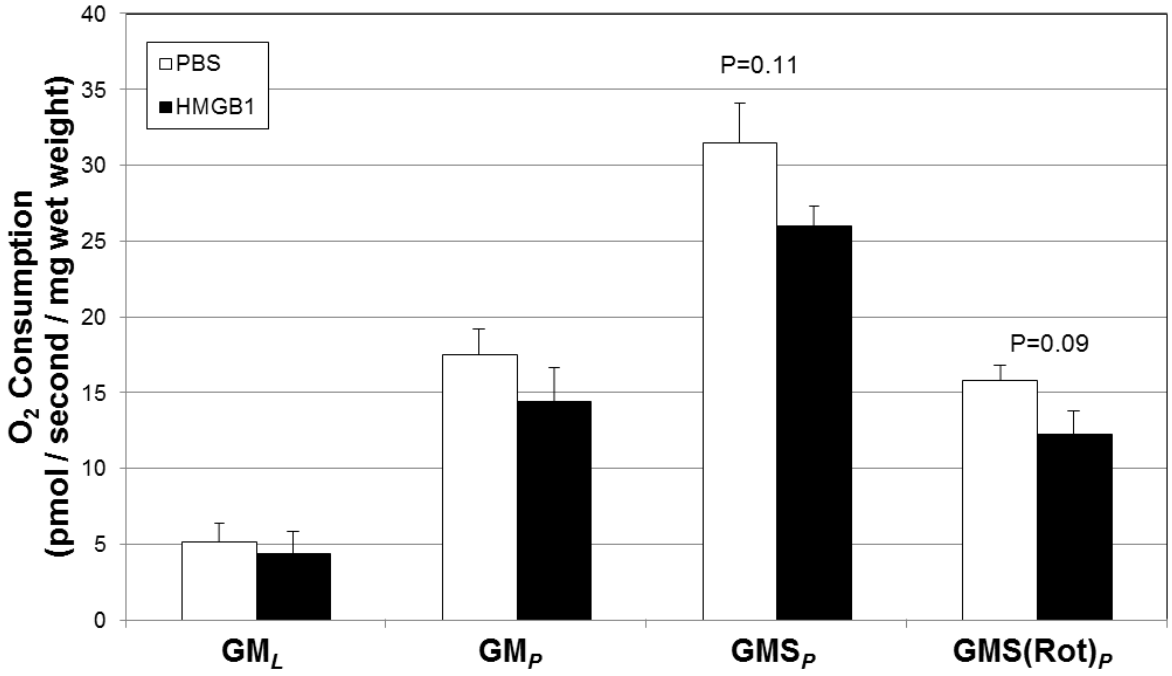

Figure 3.8: Exogenous HMGB1 And Mitochondrial Respiration In Skeletal Muscle.

Adult male C57Bl6 mice were injected with HMGB1 or vehicle daily for 2 wk. Mitochondrial respiration was analyzed in red gastrocnemius according to the protocol outlined in Methods.

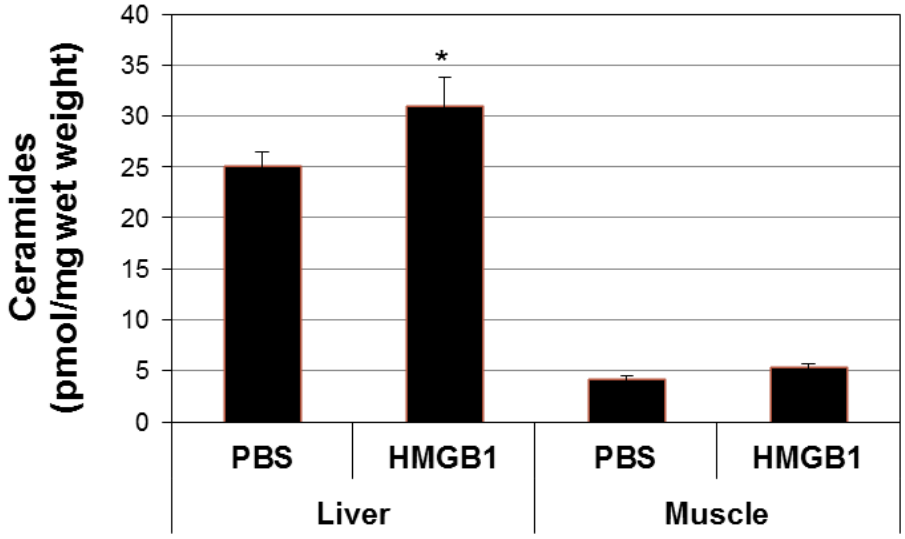

Figure 3.9: Exogenous HMGB1 Causes Increased Ceramide Accumulation In Liver.

CHAPTER 4: Conclusions

While cigarette smoking is gradually declining in the United States, it is increasing in many developing nations. Social norms and misconceptions couple with nicotine addiction to allow smoking to continue to cause deaths via heart disease, stroke, airway infections, and diabetes. Meanwhile, rates of obesity and related morbidities are climbing worldwide. While cigarette smoking has long been considered an important risk factor for type 2 diabetes, the causal relationship and molecular pathway have remained mysterious. This dissertation sought to address the following questions:

1) Can cigarette smoking alone cause metabolic disruption in mice?
2) Is ceramide involved in cigarette smoke-induced metabolic disruption?
3) What connects smoking to ceramide upregulation?

We hypothesized that cigarette smoking was sufficient to cause insulin resistance in mice and that blocking ceramide production would suspend the metabolic consequences. From there, we sought out a molecule that is likely part of this pathway, due to its association with inflammatory and insulin-resistant states and tested whether it was sufficient to induce similar metabolic disruption to cigarette smoking. The resulting studies provided the following answers to the above-mentioned questions.

Cigarette Smoking Causes Metabolic Disruption via Ceramides

In mice exposed to cigarette smoke for 8 weeks, we saw decreased sensitivity to insulin, decreased mitochondrial respiration, and increased weight gain. These markers of metabolic disruption were exacerbated by a high-fat, high-sugar diet. We also observed increased levels of ceramides and ceramide biosynthesis genes. Just as diet-induced metabolic disruption can be prevented by blocking ceramide synthesis, cigarette smoke-induced changes were reversed with

myriocin treatment. However, the combined impact of a high-fat, high-sugar diet and cigarette smoke could not be overcome with our standard dose of myriocin. This suggests that these two factors have an additive effect on metabolism and operate, at least in part, through a shared ceramide mechanism.

Exogenous HMGB1 Causes Metabolic Disruption

Because HMGB1 activates TLR4 just as saturated fat does and because HMGB1 is a RAGE ligand that is increased in lung and muscle cells during smoke exposure, HMGB1 became our next molecule of interest in bridging the gap between tobacco smoke and metabolic disruption. We found that HMGB1 injections caused insulin resistance in mice, even though we did not see any weight gain in our short two-week treatment course. Respiration in red gastrocnemius was not significantly different from control to treatment group, but myriocin increased respiration significantly from HMGB1 alone *in vitro.* A higher *in vivo* concentration of HMGB1 caused increased oxidative stress, which was alleviated by myriocin. Further evidence that HMGB1 may work through increasing ceramides was the observation that the gene transcript for Spt2, the rate-limiting enzyme for ceramide synthesis, was increased two-fold in HMGB1 muscle. To confirm HMGB1s role, HMGB1 could be blocked by a variety of small-molecules and animals could be exposed to smoke. Additionally, the cooperation of HMGB1 and ceramide could be confirmed by giving injections of both myriocin and HMGB1 to the same group of mice and comparing to either alone.

In conclusion, cigarette smoking does cause metabolic dysfunction. While there are probably many ways by which this happens, we have solid evidence that ceramide plays a role. We have also described a mechanism in which extracellular HMGB1 might be an active participant. HMGB1 is a useful target in many inflammatory conditions because of its place as a

late inflammatory signal—the same may prove true in a variety of metabolic diseases. We do not yet have a safe pharmacological inhibitor of ceramide synthesis for humans, but many effective HMGB1 inhibitors exist already and may serve as productive therapies.

REFERENCES

(2010). "Vital signs: nonsmokers' exposure to secondhand smoke -- United States, 1999-2008." MMWR Morb Mortal Wkly Rep **59**(35): 1141-1146.

(2011). "Results from the 2010 National Survey on Drug Use and Health: Summary of National Findings." Substance Abuse and Mental Health Services Administration.

Agarwal, A. R., F. Yin, et al. (2014). "Short-term cigarette smoke exposure leads to metabolic alterations in lung alveolar cells." Am J Respir Cell Mol Biol **51**(2): 284-293.

Agarwal, A. R., F. Yin, et al. (2014). "Short-term cigarette smoke exposure leads to metabolic alterations in lung alveolar cells." Am J Respir Cell Mol Biol.

Amati, F., J. J. Dube, et al. (2011). "Skeletal muscle triglycerides, diacylglycerols, and ceramides in insulin resistance: another paradox in endurance-trained athletes?" Diabetes **60**(10): 2588-2597.

Andersen, Z. J., O. Raaschou-Nielsen, et al. (2012). "Diabetes incidence and long-term exposure to air pollution: a cohort study." Diabetes Care **35**(1): 92-98.

Attvall, S., J. Fowelin, et al. (1993). "Smoking induces insulin resistance--a potential link with the insulin resistance syndrome." J Intern Med **233**(4): 327-332.

Azzalini, L., E. Ferrer, et al. (2010). "Cigarette smoking exacerbates nonalcoholic fatty liver disease in obese rats." Hepatology **51**(5): 1567-1576.

Bailey, S. M., S. K. Mantena, et al. (2009). "Ethanol and tobacco smoke increase hepatic steatosis and hypoxia in the hypercholesterolemic apoE(-/-) mouse: implications for a "multihit" hypothesis of fatty liver disease." Free Radic Biol Med **46**(7): 928-938.

Bamia, C., A. Trichopoulou, et al. (2004). "Tobacco smoking in relation to body fat mass and distribution in a general population sample." Int J Obes Relat Metab Disord **28**(8): 1091-1096.

Barnard, R. J., C. K. Roberts, et al. (1998). "Diet-induced insulin resistance precedes other aspects of the metabolic syndrome." J Appl Physiol (1985) **84**(4): 1311-1315.

Barnes, P. J. and M. Karin (1997). "Nuclear factor-kappaB: a pivotal transcription factor in chronic inflammatory diseases." N Engl J Med **336**(15): 1066-1071.

Barreiro, E., L. del Puerto-Nevado, et al. (2012). "Cigarette smoke-induced oxidative stress in skeletal muscles of mice." Respir Physiol Neurobiol **182**(1): 9-17.

Barrett-Connor, E. and K. T. Khaw (1989). "Cigarette smoking and increased central adiposity." Ann Intern Med **111**(10): 783-787.

Barton, D. B., B. C. Betteridge, et al. (2014). "Primary alveolar macrophages exposed to diesel particulate matter increase RAGE expression and activate RAGE signaling." Cell Tissue Res **358**(1): 229-238.

Bergman, B. C., L. Perreault, et al. (2012). "Novel and reversible mechanisms of smoking-induced insulin resistance in humans." Diabetes **61**(12): 3156-3166.

Bieberich, E. (2011). "There is more to a lipid than just being a fat: sphingolipid-guided differentiation of oligodendroglial lineage from embryonic stem cells." Neurochem Res **36**(9): 1601-1611.

Bierhaus, A., P. M. Humpert, et al. (2005). "Understanding RAGE, the receptor for advanced glycation end products." J Mol Med (Berl) **83**(11): 876-886.

Bierhaus, A., S. Schiekofer, et al. (2001). "Diabetes-associated sustained activation of the transcription factor nuclear factor-kappaB." Diabetes **50**(12): 2792-2808.

Bikman, B. T. (2012). "A role for sphingolipids in the pathophysiology of obesity-induced inflammation." Cell Mol Life Sci **69**(13): 2135-2146.

Bikman, B. T., Y. Guan, et al. (2012). "Fenretinide prevents lipid-induced insulin resistance by blocking ceramide biosynthesis." J Biol Chem **287**(21): 17426-17437.

Bikman, B. T. and S. A. Summers (2011). "Ceramides as modulators of cellular and whole-body metabolism." J Clin Invest **121**(11): 4222-4230.

Bonaldi, T., F. Talamo, et al. (2003). "Monocytic cells hyperacetylate chromatin protein HMGB1 to redirect it towards secretion." EMBO J **22**(20): 5551-5560.

Borissova, A. M., T. Tankova, et al. (2004). "The effect of smoking on peripheral insulin sensitivity and plasma endothelin level." Diabetes Metab **30**(2): 147-152.

Boyle, J. P., T. J. Thompson, et al. (2010). "Projection of the year 2050 burden of diabetes in the US adult population: dynamic modeling of incidence, mortality, and prediabetes prevalence." Popul Health Metr **8**: 29.

Bray, G. A. and C. M. Champagne (2005). "Beyond energy balance: there is more to obesity than kilocalories." J Am Diet Assoc **105**(5 Suppl 1): S17-23.

Brett, J., A. M. Schmidt, et al. (1993). "Survey of the distribution of a newly characterized receptor for advanced glycation end products in tissues." Am J Pathol **143**(6): 1699-1712.

Brook, R. D., M. Jerrett, et al. (2008). "The relationship between diabetes mellitus and traffic-related air pollution." J Occup Environ Med **50**(1): 32-38.

Bucciarelli, L. G., T. Wendt, et al. (2002). "RAGE is a multiligand receptor of the immunoglobulin superfamily: implications for homeostasis and chronic disease." Cell Mol Life Sci **59**(7): 1117-1128.

Cai, D., M. Yuan, et al. (2005). "Local and systemic insulin resistance resulting from hepatic activation of IKK-beta and NF-kappaB." Nat Med **11**(2): 183-190.

Carlson, M. G. and P. J. Campbell (1993). "Intensive insulin therapy and weight gain in IDDM." Diabetes **42**(12): 1700-1707.

CDCP (2014). "The Health Consequences of Smoking—50 Years of Progress: A Report of the Surgeon General."

Chavez, J. A., T. A. Knotts, et al. (2003). "A role for ceramide, but not diacylglycerol, in the antagonism of insulin signal transduction by saturated fatty acids." J Biol Chem **278**(12): 10297-10303.

Chen, C. C., T. C. Li, et al. (2008). "Association among cigarette smoking, metabolic syndrome, and its individual components: the metabolic syndrome study in Taiwan." Metabolism **57**(4): 544-548.

Chen, H., R. Vlahos, et al. (2005). "Effect of short-term cigarette smoke exposure on body weight, appetite and brain neuropeptide Y in mice." Neuropsychopharmacology **30**(4): 713-719.

Chen, M., W. Huang, et al. (2014). "High-mobility group box 1 exacerbates CCl(4)-induced acute liver injury in mice." Clin Immunol **153**(1): 56-63.

Chiolero, A., D. Faeh, et al. (2008). "Consequences of smoking for body weight, body fat distribution, and insulin resistance." Am J Clin Nutr **87**(4): 801-809.

Clowes, G. H., H. Martin, et al. (1978). "Blood insulin responses to blood glucose levels in high output sepsis and spetic shock." Am J Surg **135**(4): 577-583.

Contreras, F. X., A. V. Villar, et al. (2003). "Sphingomyelinase activity causes transbilayer lipid translocation in model and cell membranes." J Biol Chem **278**(39): 37169-37174.

Cox, J. E. and T. L. Powley (1977). "Development of obesity in diabetic mice pair-fed with lean siblings." J Comp Physiol Psychol **91**(2): 347-358.

DeFronzo, R. A. and E. Ferrannini (1991). "Insulin resistance. A multifaceted syndrome responsible for NIDDM, obesity, hypertension, dyslipidemia, and atherosclerotic cardiovascular disease." Diabetes Care **14**(3): 173-194.

Dijkema, M. B., S. F. Mallant, et al. (2011). "Long-term exposure to traffic-related air pollution and type 2 diabetes prevalence in a cross-sectional screening-study in the Netherlands." Environ Health **10**: 76.

Dominguez, H., H. Storgaard, et al. (2005). "Metabolic and vascular effects of tumor necrosis factor-alpha blockade with etanercept in obese patients with type 2 diabetes." J Vasc Res **42**(6): 517-525.

Du, J., Y. Wang, et al. (2009). "Dynamic regulation of mitochondrial function by glucocorticoids." Proceedings of the National Academy of Sciences of the United States of America **106**(9): 3543-3548.

Ebersbach-Silva, P., T. Alves, et al. (2013). "Cigarette smoke exposure severely reduces peripheral insulin sensitivity without changing GLUT4 expression in oxidative muscle of Wistar rats." Arq Bras Endocrinol Metabol **57**(1): 19-26.

Ebstein, W. (2002). "Invited comment on W. Ebstein: On the therapy of diabetes mellitus, in particular on the application of sodium salicylate." J Mol Med (Berl) **80**(10): 618; discussion 619.

Eliasson, B., S. Attvall, et al. (1994). "The insulin resistance syndrome in smokers is related to smoking habits." Arterioscler Thromb **14**(12): 1946-1950.

Eliasson, B., N. Mero, et al. (1997). "The insulin resistance syndrome and postprandial lipid intolerance in smokers." Atherosclerosis **129**(1): 79-88.

Erickson, K. A., M. E. Smith, et al. (2012). "AICAR inhibits ceramide biosynthesis in skeletal muscle." Diabetol Metab Syndr **4**(1): 45.

Eriksen (2012). "The Tobacco Atlas." Booklist **109**(4): 33-33.

Facchini, F. S., C. B. Hollenbeck, et al. (1992). "Insulin resistance and cigarette smoking." Lancet **339**(8802): 1128-1130.

Gannon, A. M., M. R. Stampfli, et al. (2013). "Cigarette smoke exposure elicits increased autophagy and dysregulation of mitochondrial dynamics in murine granulosa cells." Biol Reprod **88**(3): 63.

Gardella, S., C. Andrei, et al. (2002). "The nuclear protein HMGB1 is secreted by monocytes via a non-classical, vesicle-mediated secretory pathway." EMBO Rep **3**(10): 995-1001.

Goldkorn, T. and S. Filosto (2010). "Lung injury and cancer: Mechanistic insights into ceramide and EGFR signaling under cigarette smoke." Am J Respir Cell Mol Biol **43**(3): 259-268.

Gonzalez-Gay, M. A., J. M. De Matias, et al. (2006). "Anti-tumor necrosis factor-alpha blockade improves insulin resistance in patients with rheumatoid arthritis." Clin Exp Rheumatol **24**(1): 83-86.

Goodwin, G. H., C. Sanders, et al. (1973). "A new group of chromatin-associated proteins with a high content of acidic and basic amino acids." Eur J Biochem **38**(1): 14-19.

Gougeon, M. L. and M. Bras (2011). "Natural killer cells, dendritic cells, and the alarmin high-mobility group box 1 protein: a dangerous trio in HIV-1 infection?" Curr Opin HIV AIDS **6**(5): 364-372.

Gudz, T. I., K. Y. Tserng, et al. (1997). "Direct inhibition of mitochondrial respiratory chain complex III by cell-permeable ceramide." J Biol Chem **272**(39): 24154-24158.

Haffner, S. M., R. A. Valdez, et al. (1992). "Prospective analysis of the insulin-resistance syndrome (syndrome X)." Diabetes **41**(6): 715-722.

Hamabe, A., H. Uto, et al. (2011). "Impact of cigarette smoking on onset of nonalcoholic fatty liver disease over a 10-year period." J Gastroenterol **46**(6): 769-778.

Hanada, K., M. Nishijima, et al. (2000). "Specificity of inhibitors of serine palmitoyltransferase (SPT), a key enzyme in sphingolipid biosynthesis, in intact cells. A novel evaluation system using an SPT-defective mammalian cell mutant." Biochem Pharmacol **59**(10): 1211-1216.

Hardman, C. H., R. W. Broadhurst, et al. (1995). "Structure of the A-domain of HMG1 and its interaction with DNA as studied by heteronuclear three- and four-dimensional NMR spectroscopy." Biochemistry **34**(51): 16596-16607.

Haslam, D. W. and W. P. James (2005). "Obesity." Lancet **366**(9492): 1197-1209.

Hebert, J. R. and G. C. Kabat (1990). "Differences in dietary intake associated with smoking status." Eur J Clin Nutr **44**(3): 185-193.

Hofstetter, A., Y. Schutz, et al. (1986). "Increased 24-hour energy expenditure in cigarette smokers." N Engl J Med **314**(2): 79-82.

Hojjati, M. R., Z. Li, et al. (2005). "Effect of myriocin on plasma sphingolipid metabolism and atherosclerosis in apoE-deficient mice." J Biol Chem **280**(11): 10284-10289.

Holland, W. L., B. T. Bikman, et al. (2011). "Lipid-induced insulin resistance mediated by the proinflammatory receptor TLR4 requires saturated fatty acid-induced ceramide biosynthesis in mice." J Clin Invest **121**(5): 1858-1870.

Holland, W. L., T. A. Knotts, et al. (2007). "Lipid mediators of insulin resistance." Nutr Rev **65**(6 Pt 2): S39-46.

Hori, O., J. Brett, et al. (1995). "The receptor for advanced glycation end products (RAGE) is a cellular binding site for amphoterin. Mediation of neurite outgrowth and co-expression of rage and amphoterin in the developing nervous system." J Biol Chem **270**(43): 25752-25761.

Hotamisligil, G. S., P. Arner, et al. (1995). "Increased adipose tissue expression of tumor necrosis factor-alpha in human obesity and insulin resistance." J Clin Invest **95**(5): 2409-2415.

Hotamisligil, G. S., N. S. Shargill, et al. (1993). "Adipose expression of tumor necrosis factor-alpha: direct role in obesity-linked insulin resistance." Science **259**(5091): 87-91.

Hreggvidsdottir, H. S., T. Ostberg, et al. (2009). "The alarmin HMGB1 acts in synergy with endogenous and exogenous danger signals to promote inflammation." J Leukoc Biol **86**(3): 655-662.

Hundal, R. S., K. F. Petersen, et al. (2002). "Mechanism by which high-dose aspirin improves glucose metabolism in type 2 diabetes." J Clin Invest **109**(10): 1321-1326.

Hustvedt, B. E. and A. Lovo (1972). "Correlation between hyperinsulinemia and hyperphagia in rats with ventromedial hypothalamic lesions." Acta Physiol Scand **84**(1): 29-33.

Iochida, L. C., M. Tominaga, et al. (1989). "Insulin resistance in septic rats--a study by the euglycemic clamp technique." Life Sci **45**(17): 1567-1573.

Ito, I., J. Fukazawa, et al. (2007). "Post-translational methylation of high mobility group box 1 (HMGB1) causes its cytoplasmic localization in neutrophils." J Biol Chem **282**(22): 16336-16344.

Jee, S. H., S. Y. Lee, et al. (2002). "Effect of smoking on the paradox of high waist-to-hip ratio and low body mass index." Obes Res **10**(9): 891-895.

Jha, P. (2009). "Avoidable global cancer deaths and total deaths from smoking." Nat Rev Cancer **9**(9): 655-664.

Jheng, H. F., P. J. Tsai, et al. (2012). "Mitochondrial fission contributes to mitochondrial dysfunction and insulin resistance in skeletal muscle." Mol Cell Biol **32**(2): 309-319.

Jo, J., O. Gavrilova, et al. (2009). "Hypertrophy and/or Hyperplasia: Dynamics of Adipose Tissue Growth." PLoS Comput Biol **5**(3): e1000324.

John, U., M. Hanke, et al. (2005). "Smoking status, cigarettes per day, and their relationship to overweight and obesity among former and current smokers in a national adult general population sample." Int J Obes (Lond) **29**(10): 1289-1294.

Kawai, M., F. J. de Paula, et al. (2012). "New insights into osteoporosis: the bone-fat connection." J Intern Med **272**(4): 317-329.

Kern, P. A., M. Saghizadeh, et al. (1995). "The expression of tumor necrosis factor in human adipose tissue. Regulation by obesity, weight loss, and relationship to lipoprotein lipase." J Clin Invest **95**(5): 2111-2119.

King, B. M., R. L. Smith, et al. (1984). "Hyperinsulinemia in rats with ventromedial hypothalamic lesions: role of hyperphagia." Behav Neurosci **98**(1): 152-155.

Knight-Lozano, C. A., C. G. Young, et al. (2002). "Cigarette smoke exposure and hypercholesterolemia increase mitochondrial damage in cardiovascular tissues." Circulation **105**(7): 849-854.

Krämer, U., C. Herder, et al. (2010). "Traffic-related air pollution and incident type 2 diabetes: results from the SALIA cohort study." Environ Health Perspect **118**(9): 1273-1279.

Kuipers, M. T., T. van der Poll, et al. (2011). "Bench-to-bedside review: Damage-associated molecular patterns in the onset of ventilator-induced lung injury." Crit Care **15**(6): 235.

Levy, M., E. Khan, et al. (2009). "Neutral sphingomyelinase 2 is activated by cigarette smoke to augment ceramide-induced apoptosis in lung cell death." Am J Physiol Lung Cell Mol Physiol **297**(1): L125-133.

Li, J. and A. M. Schmidt (1997). "Characterization and functional analysis of the promoter of RAGE, the receptor for advanced glycation end products." J Biol Chem **272**(26): 16498-16506.

Makimattila, S., K. Nikkila, et al. (1999). "Causes of weight gain during insulin therapy with and without metformin in patients with Type II diabetes mellitus." Diabetologia **42**(4): 406-412.

Miro, O., J. R. Alonso, et al. (1999). "Smoking disturbs mitochondrial respiratory chain function and enhances lipid peroxidation on human circulating lymphocytes." Carcinogenesis **20**(7): 1331-1336.

Miyake, Y., Y. Kozutsumi, et al. (1995). "Serine palmitoyltransferase is the primary target of a sphingosine-like immunosuppressant, ISP-1/myriocin." Biochem Biophys Res Commun **211**(2): 396-403.

Müller, S., P. Scaffidi, et al. (2001). "New EMBO members' review: the double life of HMGB1 chromatin protein: architectural factor and extracellular signal." EMBO J **20**(16): 4337-4340.

Musumeci, D., G. N. Roviello, et al. (2014). "An overview on HMGB1 inhibitors as potential therapeutic agents in HMGB1-related pathologies." Pharmacol Ther **141**(3): 347-357.

Naruse, K., T. Sado, et al. (2012). "Peripheral RAGE (receptor for advanced glycation endproducts)-ligands in normal pregnancy and preeclampsia: novel markers of inflammatory response." J Reprod Immunol **93**(2): 69-74.

Ni, X. R., Z. J. Sun, et al. (2015). "High concentration of insulin promotes apoptosis of primary cultured rat ovarian granulosa cells via its increase in extracellular HMGB1." Reprod Sci **22**(3): 271-277.

Pearson, J. F., C. Bachireddy, et al. (2010). "Association between fine particulate matter and diabetes prevalence in the U.S." Diabetes Care **33**(10): 2196-2201.

Pesta, D. and E. Gnaiger (2012). "High-resolution respirometry: OXPHOS protocols for human cells and permeabilized fibers from small biopsies of human muscle." Methods Mol Biol **810**: 25-58.

Pfaffl, M. W. (2001). "A new mathematical model for relative quantification in real-time RT-PCR." Nucleic Acids Res **29**(9): e45.

Pickup, J. C. and M. A. Crook (1998). "Is type II diabetes mellitus a disease of the innate immune system?" Diabetologia **41**(10): 1241-1248.

Pirkle, J. L., J. T. Bernert, et al. (2006). "Trends in the exposure of nonsmokers in the U.S. population to secondhand smoke: 1988-2002." Environ Health Perspect **114**(6): 853-858.

Pirkle, J. L., K. M. Flegal, et al. (1996). "Exposure of the US population to environmental tobacco smoke: the Third National Health and Nutrition Examination Survey, 1988 to 1991." JAMA **275**(16): 1233-1240.

Qin, Y. H., S. M. Dai, et al. (2009). "HMGB1 enhances the proinflammatory activity of lipopolysaccharide by promoting the phosphorylation of MAPK p38 through receptor for advanced glycation end products." J Immunol **183**(10): 6244-6250.

Raij, L., E. G. DeMaster, et al. (2001). "Cigarette smoke-induced endothelium dysfunction: role of superoxide anion." J Hypertens **19**(5): 891-897.

Rajagopalan, S. and R. D. Brook (2012). "Air pollution and type 2 diabetes: mechanistic insights." Diabetes **61**(12): 3037-3045.

Raymond, R. M., J. M. Harkema, et al. (1981). "Skeletal muscle insulin resistance during Escherichia coli bacteremic shock in the dog." Surgery **90**(5): 853-859.

Read, C. M., P. D. Cary, et al. (1993). "Solution structure of a DNA-binding domain from HMG1." Nucleic Acids Res **21**(15): 3427-3436.

Reaven, G. and P. S. Tsao (2003). "Insulin resistance and compensatory hyperinsulinemia: the key player between cigarette smoking and cardiovascular disease?" J Am Coll Cardiol **41**(6): 1044-1047.

Reaven, G. M. and Y. D. Chen (1992). "Insulin resistance and cigarette smoking." Lancet **340**(8815): 377.

Reynolds, P. R., M. G. Cosio, et al. (2006). "Cigarette smoke-induced Egr-1 upregulates proinflammatory cytokines in pulmonary epithelial cells." Am J Respir Cell Mol Biol **35**(3): 314-319.

Reynolds, P. R., S. D. Kasteler, et al. (2008). "RAGE: developmental expression and positive feedback regulation by Egr-1 during cigarette smoke exposure in pulmonary epithelial cells." Am J Physiol Lung Cell Mol Physiol **294**(6): L1094-1101.

Reynolds, P. R., S. D. Kasteler, et al. (2011). "Receptor for advanced glycation end-products signals through Ras during tobacco smoke-induced pulmonary inflammation." Am J Respir Cell Mol Biol **45**(2): 411-418.

Robinson, A. B., J. A. Stogsdill, et al. (2012). "RAGE and tobacco smoke: insights into modeling chronic obstructive pulmonary disease." Front Physiol **3**: 301.

Scaffidi, P., T. Misteli, et al. (2002). "Release of chromatin protein HMGB1 by necrotic cells triggers inflammation." Nature **418**(6894): 191-195.

Schmidt, A. M., S. D. Yan, et al. (2001). "The multiligand receptor RAGE as a progression factor amplifying immune and inflammatory responses." J Clin Invest **108**(7): 949-955.

Schmitz-Peiffer, C. (2002). "Protein kinase C and lipid-induced insulin resistance in skeletal muscle." Ann N Y Acad Sci **967**: 146-157.

Semino, C., G. Angelini, et al. (2005). "NK/iDC interaction results in IL-18 secretion by DCs at the synaptic cleft followed by NK cell activation and release of the DC maturation factor HMGB1." Blood **106**(2): 609-616.

Shangraw, R. E., F. Jahoor, et al. (1989). "Differentiation between septic and postburn insulin resistance." Metabolism **38**(10): 983-989.

Shier, W. T., Shier A.C. (2000). "Sphingosine and ceramide-analog toxins—an update." Journal of Toxicology(Toxin Reviews): 189-246.

Shimokata, H., D. C. Muller, et al. (1989). "Studies in the distribution of body fat. III. Effects of cigarette smoking." JAMA **261**(8): 1169-1173.

Shoelson, S. E., J. Lee, et al. (2003). "Inflammation and the IKK beta/I kappa B/NF-kappa B axis in obesity- and diet-induced insulin resistance." Int J Obes Relat Metab Disord **27 Suppl 3**: S49-52.

Simon, J. A., D. G. Seeley, et al. (1997). "The relation of smoking to waist-to-hip ratio and diabetes mellitus among elderly women." Prev Med **26**(5 Pt 1): 639-644.

Sims, G. P., D. C. Rowe, et al. (2010). "HMGB1 and RAGE in inflammation and cancer." Annu Rev Immunol **28**: 367-388.

Smith, M. E., T. S. Tippetts, et al. (2013). "Mitochondrial fission mediates ceramide-induced metabolic disruption in skeletal muscle." Biochem J **456**(3): 427-439.

Smith, P. R., J. M. Cooper, et al. (1993). "Smoking and mitochondrial function: a model for environmental toxins." Q J Med **86**(10): 657-660.

Sonmez, A., T. Dogru, et al. (2006). "Adiponectin and insulin resistance in young and healthy smokers." Endocr J **53**(6): 729-734.

Speizer, F. E. (1992). "Getting some breathing room--persuading patients to stop smoking." West J Med **157**(5): 585-586.

Summers, S. A. (2006). "Ceramides in insulin resistance and lipotoxicity." Prog Lipid Res **45**(1): 42-72.

Thatcher, M. O., T. S. Tippetts, et al. (2014). "Ceramides mediate cigarette smoke-induced metabolic disruption in mice." Am J Physiol Endocrinol Metab **307**(10): E919-927.

Thomas, J. O. (2001). "HMG1 and 2: architectural DNA-binding proteins." Biochem Soc Trans **29**(Pt 4): 395-401.

Tian, J., A. M. Avalos, et al. (2007). "Toll-like receptor 9-dependent activation by DNA-containing immune complexes is mediated by HMGB1 and RAGE." Nat Immunol **8**(5): 487-496.

Tong, M., L. Longato, et al. (2014). "Therapeutic reversal of chronic alcohol-related steatohepatitis with the ceramide inhibitor myriocin." Int J Exp Pathol **95**(1): 49-63.

Torbay, N., E. F. Bracco, et al. (1985). "Insulin increases body fat despite control of food intake and physical activity." Am J Physiol **248**(1 Pt 2): R120-124.

Treutiger, C. J., G. E. Mullins, et al. (2003). "High mobility group 1 B-box mediates activation of human endothelium." J Intern Med **254**(4): 375-385.

Troost, J. P., D. A. Barondess, et al. (2012). "An updated global picture of cigarette smoking persistence among adults." J Epidemiol Glob Health **2**(3): 135-144.

Turban, S. and E. Hajduch (2011). "Protein kinase C isoforms: mediators of reactive lipid metabolites in the development of insulin resistance." FEBS Lett **585**(2): 269-274.

Turinsky, J., B. P. Bayly, et al. (1990). "1,2-Diacylglycerol and ceramide levels in rat skeletal muscle and liver in vivo. Studies with insulin, exercise, muscle denervation, and vasopressin." J Biol Chem **265**(14): 7933-7938.

Valdes-Ferrer, S. I., M. Rosas-Ballina, et al. (2013). "HMGB1 mediates splenomegaly and expansion of splenic CD11b+ Ly-6C(high) inflammatory monocytes in murine sepsis survivors." J Intern Med **274**(4): 381-390.

Velasquez-Mieyer, P. A., P. A. Cowan, et al. (2003). "Suppression of insulin secretion is associated with weight loss and altered macronutrient intake and preference in a subset of obese adults." Int J Obes Relat Metab Disord **27**(2): 219-226.

Visser, M., L. M. Bouter, et al. (1999). "Elevated C-reactive protein levels in overweight and obese adults." JAMA **282**(22): 2131-2135.

Vlassara, H., M. Brownlee, et al. (1985). "High-affinity-receptor-mediated uptake and degradation of glucose-modified proteins: a potential mechanism for the removal of senescent macromolecules." Proc Natl Acad Sci U S A **82**(17): 5588-5592.

Vlassara, H., R. Bucala, et al. (1994). "Pathogenic effects of advanced glycosylation: biochemical, biologic, and clinical implications for diabetes and aging." Lab Invest **70**(2): 138-151.

Wang, H., O. Bloom, et al. (1999). "HMG-1 as a late mediator of endotoxin lethality in mice." Science **285**(5425): 248-251.

Wang, Q., M. Zeng, et al. (2007). "The HMGB1 acidic tail regulates HMGB1 DNA binding specificity by a unique mechanism." Biochem Biophys Res Commun **360**(1): 14-19.

Watt, M. J., A. C. Barnett, et al. (2012). "Regulation of plasma ceramide levels with fatty acid oversupply: evidence that the liver detects and secretes de novo synthesised ceramide." Diabetologia **55**(10): 2741-2746.

Weir, H. M., P. J. Kraulis, et al. (1993). "Structure of the HMG box motif in the B-domain of HMG1." EMBO J **12**(4): 1311-1319.

Williamson, R. T. (1901). "On the Treatment of Glycosuria and Diabetes Mellitus with Sodium Salicylate." Br Med J **1**(2100): 760-762.

World Health Organization, W. (2012). "Obesity and Overweight." http://www.who.int/mediacentre/factsheets/fs311/en/ **Fact Sheet 311**.

Wright, J. L., M. Cosio, et al. (2008). "Animal models of chronic obstructive pulmonary disease." Am J Physiol Lung Cell Mol Physiol **295**(1): L1-15.

Yuan, M., N. Konstantopoulos, et al. (2001). "Reversal of obesity- and diet-induced insulin resistance with salicylates or targeted disruption of Ikkbeta." Science **293**(5535): 1673-1677.

Yudkin, J. S. (2000). "Relationship of serum C3 complement with insulin resistance and coronary heart disease-cause, consequence or common antecedent?" Eur Heart J **21**(13): 1036-1039.

CURRICULUM VITAE

MIKAYLA ORTON THATCHER
159 E 300S #2 Provo, UT 84606

EDUCATION

Brigham Young University
Ph. D. in Physiology and Developmental Biology 2015
Dissertation: HMGB1 and Ceramides: Potential Mediators of Cigarette Smoke-Induced Metabolic Dysfunction

Brigham Young University
B. S. in Physiology and Developmental Biology 2011

RESEARCH EXPERIENCE

Graduate Research Assistant 2012-2015
Dr. Benjamin Bikman, Mentor

Research Technician at Myriad Genetics 2011-2012

Undergraduate Mentored Research 2009-2011
Dr. John Bell, Mentor

TEACHING EXPERIENCE

Nursing Department
Ameritech College of Healthcare
Instructor for Pathophysiology 240 2015

Biology Department
Brigham Young University
Instructor for Biology 100 2015
Biology Education Fellow 2014

Department of Physiology and Developmental Biology
Brigham Young University
Teaching Assistant— PDBio 305 "Physiology" 2012-2015
PDBio 362 "Advanced Physiology"
PDBio 363 "Advanced Physiology Lab"
PDBio 365 "Pathophysiology"
Attended class to explain concepts and answer student questions; held weekly office hours; taught homework and exam review sessions

Teaching Practicum—PDBio 305 "Physiology" 2013
Dr. David Thomson, Supervisor
Designed and taught 9 lectures to a class of thirty students, wrote quiz and exam questions

Teaching Practicum—PDBio 305 "Physiology" 2013
Dr. Roy Silcox, Supervisor
Designed and taught eight two-hour lectures to a class of fifty students

AWARDS

Full Tuition Award 2012-2015
Department of Physiology and Developmental Biology

Research Assistantship 2011-2014
Department of Physiology and Developmental Biology

Teaching Assistantship 2011-2014
Department of Physiology and Developmental Biology

Graduate Research Fellowship 2013-2014
BYU Graduate Studies

Research Presentation Award 2013, 2014
BYU Graduate Studies

PUBLICATIONS

Investigation into the role of phosphatidylserine in modifying the susceptibility of human lymphocytes to secretory phospholipase A(2) using cells deficient in the expression of scramblase. Nelsen et al. Biochim Biophys Acta. 2012

AICAR inhibits ceramide biosynthesis in skeletal muscle. Erickson et al. Diabetol Metab Syndr. 2012

Ceramides mediate cigarette smoke-induced metabolic disruption in mice. Thatcher et al. Am J Physiol Endocrinol Metab. 2014

Cigarette smoke increases cardiomyocyte ceramide accumulation and inhibits mitochondrial respiration. Tippetts et al. BMC Cardiovasc Disord. 2014

PRESENTATIONS

Experimental Biology, 2013

American Diabetes Association, 2014